PŘÍLOHY K DISERTAČNÍ PRÁCI

SPECIAČNÍ ANALÝZA ARSENU A RTUTI POMOCÍ POSTKOLONOVÉHO GENEROVÁNÍ TĚKAVÝCH SLOUČENIN PRO POTŘEBY ATOMOVÝCH SPEKTROMETRICKÝCH METOD

Speciation analysis of arsenic and mercury using postcolumn generation of their volatile compounds for needs of atomic spectroscopic methods

SEZNAM PŘÍLOH

Součástí disertační práce jsou tři přílohy. Jedná se o články publikované v odborných časopisech (Příloha 1 - 3). Článek (Příloha 3) byl dne 29.05.2018 přijat k publikování v časopisu Analytical Letters; zde je přiložen přijatý manuskript.

1. **Linhart O.**, Smolejová J., Červený V., Hraníček J., Nováková E., Resslerová T., Rychlovský P.: Determination of As by UV-photochemical generation of its volatile species with AAS detection. Monatsh. Chem. 147, 1447-1454 (2016).
   DOI: 10.1007/s00706-016−1808-5

2. Nováková E., **Linhart O.**, Červený V., Rychlovský P., Hraníček J.: Flow injection determination of Se in dietary supplements using TiO_2, mediated ultraviolet-photochemical volatile species generation. Spectrochim. Acta, Part B 134, 98-104 (2017)
   DOI: 10.1016/j.sab.2017.06.007

3. **Linhart O.**, Mrázová-Kolorosová A., Kratzer J., Hraníček J., Červený V.: Mercury Speciation in Fish by High-Performance Liquid Chromatography (HPLC) and Post-Column Ultraviolet (UV)-Photochemical Vapor Generation (PVG): Comparison of Conventional Line-Source and High-Resolution Continuum Source (HR-CS) Atomic Absorption Spectrometry (AAS) Přijato k publikování v Analytical Letters (2018)
   DOI: 10.1080/00032719.2018.1483380

Monatsh Chem
DOI 10.1007/s00706-016-1808-5

ORIGINAL PAPER

Determination of As by UV-photochemical generation of its volatile species with AAS detection

Ondřej Linhart[1] · Jana Smolejová[1] · Václav Červený[1] · Jakub Hraníček[1] · Eliška Nováková[1] · Tina Resslerová[1] · Petr Rychlovský[1]

Received: 30 January 2016 / Accepted: 20 June 2016

Abstract This work was focused on the development of an analytical method for determination of arsenic in liquid (aqueous solutions of arsenite) by UV-photochemical generation of its volatile compounds. The study contains the optimization, method characterisation and also a study of the influence of selected compounds on the signal measured. The method involves a combination of flow injection analysis, UV-photochemical generation of volatile compounds of arsenic in flow injection arrangement and atomic absorption spectrometry using an externally heated quartz tube atomizer. The attained absorbance was very low after the optimization. In the next step, the influence of selected compounds on UV-photochemical generation was investigated with the aim to find a suitable reaction modifier that would improve the sensitivity of arsenic determination. Bi(III) was found as the best reaction modifier not only for causing the increase of the signal of arsenic measured but also for its persisting effect. The activation with concentration of 10 mg dm^{-3} of Bi(III) increases the absorbance of arsenic approximately eleven times compared to signals without activation. Following method characteristics were achieved under the optimum experimental conditions: the limit of detection of 18 μg dm^{-3}, the repeatability of 4.5 % expressed as % RSD at 200 μg dm^{-3}, and linear dynamic range 60–500 μg dm^{-3} of arsenic.

Graphical abstract

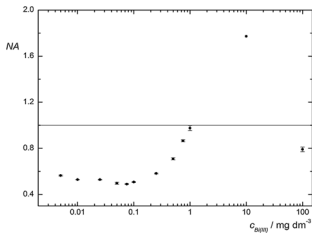

Keywords UV-photochemical generation · Arsenic · Photochemistry · Spectroscopy · Green chemistry · Ecology

Introduction

UV-photochemical generation of volatile compounds is important and well known technique in atomic spectrometry that can be used to determine metals, metalloids, or organometallic compounds. There are several approaches for conversion of the analyte from the aqueous phase into the gaseous phase. The chemical vapour generation (CVG) using borohydride as a reducing agent in the presence of mineral acid is the most popular way for the volatile compound forming elements. The common mixture is $NaBH_4$/HCl used in CVG [1, 2]. The electrochemical generation is the other method in which the electric current is used for reduction of the analyte to the volatile species in presence of mineral acid medium [3, 4]. At last, the UV-photochemical vapour generation (UV-PVG) has been used [5, 6]. It is an alternative to the two previous methods. Volatile compounds are formed under the UV irradiation in presence of low molecular weight organic acid (formic,

✉ Ondřej Linhart
linharo2@natur.cuni.cz

[1] Department of Analytical Chemistry, Faculty of Science, Charles University in Prague, Albertov 6, 128 43 Prague, Czech Republic

Published online: 26 July 2016

acetic, and propionic acid) [7–9] or other chemicals [10–12] in the UV generator. UV-photochemical generation can be combined with different detection such as AAS [13–17], AFS [10, 18–20], ICP-MS [5, 10, 18, 21, 22], ICP-OES [23, 24] or can be used as a derivatization unit for speciation analysis [20, 27–31] connected to the output of chromatographic column.

UV-photochemical generation of volatile compounds with various kinds of detection is one of the possible ways to determine arsenic [32] and also other hydride forming elements [25, 26] in the sample. This derivatization method is based on photolytic decomposition of low molecular weight organic acids (formic, acetic, propionic) to form hydrocarbons, radicals and CO_2, according to the Eq. (1) [32].

$$\mathrm{R\text{-}COOH} \xrightarrow{h\nu} \mathrm{R}^{\bullet} + {}^{\bullet}\mathrm{COOH} \rightarrow \mathrm{RH} + \mathrm{CO_2} \quad (\mathrm{R} = \mathrm{C}_n\mathrm{H}_{2n+1}, n = 0, 1, 2). \tag{1}$$

Hydrocarbon radicals are taken up by trivalent arsenic to form stable substituted compounds as shown in Eq. (2) [32].

$$3\mathrm{RCOOH} + \mathrm{H_3AsO_3} \xrightarrow{h\nu} 3\mathrm{CO_2} + \mathrm{R_3As} + 3\mathrm{H_2O} \quad (\mathrm{R} = \mathrm{C}_n\mathrm{H}_{2n+1}, n = 0, 1, 2). \tag{2}$$

For a spontaneous release of the compounds generated from a solution it is necessary that the products formed are sufficiently volatile. Such compounds containing the determined element are formed by photolysis of formic acid, acetic acid, and propionic acid. Volatile arsenic species generated by UV irradiation of aqueous solutions of arsenite in various low molecular weight carboxylic acid media are identified in article [32]. Identification of arsenic alkylation products by UV irradiation in acetic acid solution was reported in detail in paper [33]. The authors concluded that the photoalkylation of arsenic in acetic acid by UV irradiation has not only formed trimethylarsine, but also a whole range of aqueous soluble species. They also presumed similar processes for other low molecular weight carboxylic acid media.

The aim of this work was to develop a method of UV-photochemical generation of volatile compounds (UV-PVG) employable for determination of arsenic with atomic absorption detection in an externally heated quartz tube (QT-AAS) in a flow injection analysis (FIA) mode. The method is based on a reaction of formic acid with arsenic compounds by UV irradiation. We looked for ions or compounds influencing the signal measured, especially in a positive way. The suitable reaction modifier was chosen based on these results. The developed analytical method was successfully used for determination of arsenic (III) compounds in model samples as a basis for the future investigation considering of speciation analysis.

Results and discussion

It was experimentally proved that evaluation from peak heights was more precise than evaluation from peak areas in FIA mode for this study. The peaks were usually high, narrow and nearly symmetrical with very small influence of analytical zone dispersion.

Optimization of working conditions

First, it was necessary to find the optimum conditions for UV-photochemical generation of volatile arsenic compounds. Following key parameters were optimized: the volume of sampling loop, the length of irradiated reaction coil (UV-photoreactor), the flow rate of carrier liquid, the concentration of formic acid in this solution, the flow rate and input/inlet position of gases (Ar, H_2), and the temperature of the atomizer. The optimum experimental conditions were found to achieve a sufficient signals as well as the highest possible efficiency of the generation of volatile arsenic compounds. FIA instrumental set-up is introduced in Experimental part of this paper and it is shown in Fig. 6. The list of initial conditions is shown in Table 1. Each of these parameters was optimized to achieve the highest peak in FIA mode.

Influence of carrier gas flow rate connected before sampling valve

Argon was introduced as the carrier gas into the apparatus through PTFE tube and peristaltic pump. Its flow rate was controlled by the choice of suitable diameter of Tygon pumping tube. This kind of carrier gas introduction was used for segmentation of flow and prevention of spread zones of the injected sample. The tube with inner diameter of 0.51 mm and carrier liquid flow rate of 0.33 $cm^3\ min^{-1}$ were chosen as optimum values of these parameters for further measurements.

Effect of carrier gas (Ar) total flow rate

It was found experimentally that the presence of carrier gas is necessary for the efficient release of volatile compounds of arsenic from a liquid phase and for their quantitative transport into the atomizer. The effect of the carrier gas total flow rate was studied from 16 to 110 $cm^3\ min^{-1}$. It had a significant effect not only on the gas–liquid separation and on the analyte transport but the carrier gas flow rate also influenced the UV-PVG. The baseline was not stable at low values of flow rate of argon. It could have several causes. The explanation could be connected with the different composition of the gaseous phase transported from the gas–liquid separator; mixing the carrier gas with

Table 1 Working conditions for determination of arsenic by FIA-UV-PVG/QT-AAS

Parameter	Initial value	Optimized value
Total flow rate of carrier gas Ar/ cm^3 min^{-1}	50	24
Flow rate of reaction gas H_2/cm^3 min^{-1}	25	30
Flow rate of carrier liquid/cm^3 min^{-1}	2	2
Length of reaction coil/cm	250	250
Volume of injected sample/mm^3	600	600
Concentration of HCOOH/mol dm^{-3}	1.5	0.75
Temperature of atomizer/°C	950	950

reaction gas and with the oxygen diffused from atmosphere surrounding the atomizer (insufficiently shielded by Ar). The effect of argon flow rate on peak width (approximately 30 s) was not significant, whereas peak height was influenced strongly. The absorbance increased rapidly with decreasing argon flow rate. Figure 1 shows the effect of carrier gas flow rate on the signal of arsenic. The total flow rate of 24 cm^3 min^{-1} Ar was chosen for all the following experiments as the optimum.

Effect of reaction gas (H_2) flow rate

The presence of hydrogen radicals is necessary for UV-photochemical generation of volatile compounds of arsenic as well as for their atomization in the quartz tube atomizer. Therefore, it was investigated if added hydrogen into the UV-photoreactor can increase the signals (probably as well as the reaction rate) in FIA arrangement. Attained dependence is shown in Fig. 2. The absorbance first increased with the ascending hydrogen flow rate starting at 10 cm^3 min^{-1}, reached the maximum at 30 cm^3 min^{-1}, and then slowly decreased for higher flow rates. Reaction of the excess of hydrogen in the atomizer with atmospheric oxygen provided radicals as well as water and changed the atomization conditions. These changes resulted in a decrease of measured peak heights while the width was approximately constant. The introduction of the inert carrier gas instead of the reaction gas at the same flow rate by this channel did not lead to any increase of peaks.

Dependence of the absorbance (peak height) on concentration of formic acid

Aqueous formic acid solution served as carrier liquid in this analytical method. Therefore, concentration of formic acid was the next optimized parameter. It was a key parameter for UV-photochemical generation because it is a source of radicals. The appropriate concentration of formic acid is needed for generation of volatile compounds of arsenic. The samples of arsenite were prepared in the solutions containing the same concentration of formic acid, as was the concentration in carrier liquid. The best signal absorbance was attained for 0.75 mol dm^{-3}. Therefore, this concentration of formic acid was applied as an optimized condition for following experiments (Fig. 3). The optimum working conditions for the determination of arsenic by UV-photochemical generation with AAS detection are listed in Table 1.

Effect of selected compounds

A hollow cathode lamp was replaced by a Superlamp at the beginning of this part of the study with the aim to improve the signal/noise ratio.

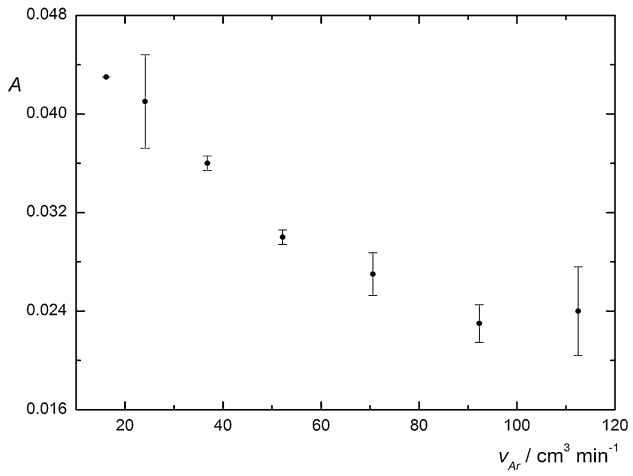

Fig. 1 Effect of argon total flow rate on the absorbance signal. Concentration of arsenic: 0.4 mg dm^{-3}. Experimental conditions are given in Table 1

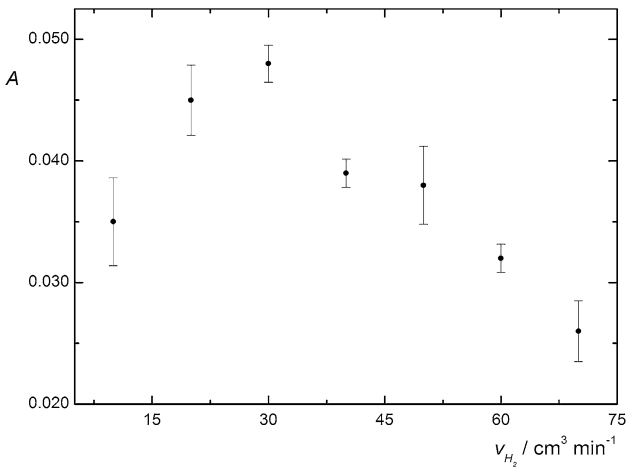

Fig. 2 Effect of hydrogen flow rate on absorbance. Concentration of arsenic: 0.4 mg dm^{-3}. Other experimental conditions are given in Table 1

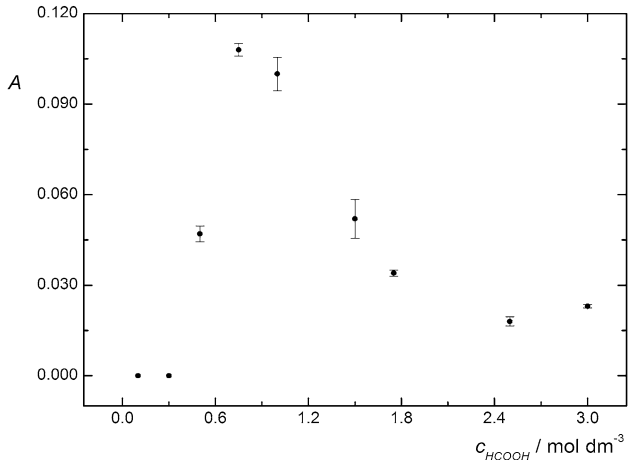

Fig. 3 Effect of concentration of formic acid (in carrier liquid). Concentration of arsenic: 1 mg dm^{-3}. Other experimental conditions are given in Table 1

It is well known that some compounds can influence the UV-photochemical generation used for determination of arsenic. The effect of fifteen various compounds or ions on the arsenic determination by UV-PVG-AAS was investigated with the intended purpose to find a suitable reaction modifier which could make UV-PVG analytically usable. It was not the aim to do a detailed overview of interferences but just to find such substances and to compare their positive effect and experimental conditions at which they would increase the arsenic absorbance. The concentration of arsenic of 1 mg dm^{-3} was used for this study in model samples as well as the appropriate concentration of the compounds or ions tested in the range from 10^{-3} to 10^{2} - mg dm^{-3}. Consequently, the signals of model samples enriched by various concentrations of selected compounds were measured.

Following substances were tested: transitions metals (Fe, Ni, Co, and Cu as common interferents for hydride generation), organic compounds (ethanol, 2-mercaptoethanol, triethanolamin, and acetonitrile as possible solvents or additives for HPLC with the intended use in speciation analysis), and other compounds [nitric acid, hydrochloric acid, sulfuric acid, titanium dioxide, L-cysteine, Se(IV), and Bi(III)] selected on the base of facts presented in published articles related to UV-PVG or to hydride generation. For example, 2-mercaptoethanol is used for UV-photochemical generation of mercury cold vapour because it increases the signal measured significantly [27, 34].

The tested compounds can be divided into three groups according to the results attained: compounds with a negative effect (in following text negative interferents), minimum interfering species and compounds with a positive effect on arsenic signal (positive interferents or potential reaction modifiers).

The higher was the concentration of each negative interferent the more intensive was the depression of arsenic signal. Negative interferents group includes: Ni(II) reducing the absorbance of arsenic more than three times from 0.01 mg dm^{-3}, Cu(II) ions which significantly reduced the signal from 0.1 mg dm^{-3}, chloride ions reducing absorbance more than a half from 0.01 mg dm^{-3}, and 2-mercaptoethanol which was the most significant negative interferent and its concentration higher than 0.005 mg dm^{-3} caused a decrease of absorbance to zero.

The minimum interfering species like nitric acid, Fe(III), ethanol, sulfate ions, titanium dioxide, and L-cysteine had just an insignificant effect on the signal of As(III) in range of 0.01–1 mg dm^{-3}. About one (HNO_3, Fe(III), ethanol, L-cysteine) or two (sulfate ions, TiO_2) order higher concentration of these substances (compared to the As(III) concentration) in model sample solutions had negative impact on arsenic absorbance which was proportional to its concentration too.

The positive interferents group includes: Co(II) increasing absorbance about 65 % in the concentration range from 0.01 to 0.1 mg dm^{-3}, acetonitrile with a positive effect (about 50 %) in the entire concentration range (from 0.005 to 100 mg dm^{-3}), triethanolamine which had a significant positive influence (about 20 %) also from 0.01 to 0.1 mg dm^{-3}, Se(IV) which interfered positively (about 35 %) in the range from 0.005 to 0.1 mg dm^{-3}, and bismuth ions which increased the absorbance most significantly at 10 mg dm^{-3}. A very strong (up to 100 %) negative influence on arsenic absorbance was observed at concentrations of these substances higher than for above listed concentration ranges with positive effect.

The most interesting results were obtained with Bi(III). The enhancement of arsenic absorbance was about 86 % in the presence of 10 mg dm^{-3} of Bi(III). This was the best result achieved. For this reason, Bi(III) was chosen as the most suitable reaction modifier for the determination of arsenic using UV-photochemical generation of volatile compounds and AAS. The influence of Bi(III) on arsenic absorbance measured is displayed in Fig. 4 as a very important example of attained dependences. The concentration of Bi(III) is plotted in a logarithmic scale on horizontal axis and the normalized absorbance (with the reference value measured previously for 1 mg dm^{-3} As(III) without the presence of any studied compound indicated by a horizontal line) on vertical axis in Fig. 4. Similarly as chloride ions or Ni(II), Bi(III) caused peak height decrease more than a half since a concentration of 5–10 μg dm^{-3}. Attained peaks became the same height as without the presence of Bi(III) when increasing its concentration to 1 mg dm^{-3}. The addition of Bi(III) above this concentration lead to increase of arsenic signal. The

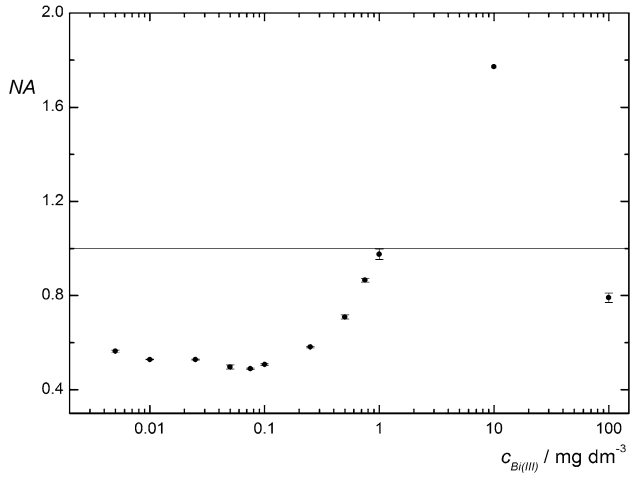

Fig. 4 Effect of Bi(III) concentration on the normalized absorbance (NA) of As. Concentration of arsenic: 1 mg dm^{-3}. Used optimum experimental conditions are listed in Table 1

presence of 100 mg dm^{-3} of Bi(III) lead to decrease of arsenic signal again.

The following experiments have shown that it is not necessary to add Bi(III) into each sample solution but it is simply enough to flush the apparatus with a solution of 10 mg dm^{-3} of Bi(III) for a few minutes before the start of the measurements. This modified apparatus was consequently stable throughout the whole day of measurements. The localization and mechanism of acting would be a subject of a future investigation.

Figures of merit

The characterisation of analytical method for As(III) determination by UV-PVG/QT-AAS was performed after all the optimization experiments. First, the calibration in the concentration range from 0 to 1.6 mg dm^{-3} of As(III) was measured without previous activation by Bi(III) under the optimum working conditions. The established values of following parameters are summarized in Table 2. Limit of detection (LOD) and limit of quantification (LOQ) were calculated as the concentration causing a signal equal to three times (or ten times, respectively) the standard deviation of ten repeated measurements of the As(III) model solution with a concentration of 200 μg dm^{-3}. The repeatability was expressed as the relative standard deviation (% RSD, $n = 10$) of results for 1.5 mg dm^{-3} of As(III). The calibration dependence is depicted in Fig. 5. The linear dynamic range (LDR) was relatively wide thanks to the low sensitivity.

Second, the calibration with long term modification (after the activation of the apparatus by Bi(III) but without addition of Bi(III) into the sample solution or carrier liquid) of the apparatus was measured again in concentration interval from 0 to 1 mg dm^{-3} of As(III). For comparison of both calibration dependences please see Fig. 5. The parameters characterizing this method were determined by the same procedure as the previous. An overview of their values is given in Table 2 for easy comparison between the approach without and after the activation. The LOD and LOQ [attained for concentration of 20 μg dm^{-3} of As(III)] moved to the lower concentration level as well as LDR after the activation. On the other hand, LDR became shorter in this case. From equations of the calibration lines, the signal enhancement factor (calculated as a ratio of both sensitivities) was calculated. Its value is 10.8.

Conclusions

A simple apparatus was constructed for determination of arsenite in model aqueous solutions by flow injection analysis. UV-photochemical vapour generation connected on-line with AAS detection in externally heated quartz tube atomizer was employed in this work. However, a very poor absorbance was attained after the optimization of the experimental conditions, which are usual for UV-PVG of other elements. Therefore, fifteen selected compounds were tested with the expectation to find a suitable reaction modifier with a positive effect for UV-photochemical generation of volatile arsenic compounds.

The most positive influence on arsenic absorbance (increase of 86 %) was observed in presence of 10 mg dm^{-3} of Bi(III) in a sample. Even more interesting is that Bi(III) became evident a long term modifier of internal surface of the apparatus. The localization and mechanism of this activity would be a subject of future investigation but it is a fact that this effect persisted for all the following measurements of the day after flushing the apparatus by the Bi(III) solution. Thus it is not needed to add Bi(III) into the routine or calibration samples.

The proposed method is distinguished by a detection limit of 18 μg dm^{-3} of arsenic, by a sensitivity of 1.1×10^{-3} dm^3 μg^{-1} (nearly 11 times higher than without activation), by a repeatability of 4.5 % and by a linear dynamic range of 60–500 μg dm^{-3} under the optimum conditions and after the activation by bismuth(III).

Relevant data for comparison of method characteristic (combination of UV-PVG with QT-AAS) were not found in available published articles. For partly comparison, limit of detection of 0.09 μg dm^{-3} (peak height) was reported for determination of arsenic by high-pressure liquid flow injection to high-resolution continuum source hydride generation atomic absorption spectrometry [35]. Just about one order lower LOD was found for arsenical speciation analysis by HPLC-(UV)-HG-AFS [29]. About one and half order lower LOD reached by the same volatile compounds

Table 2 Figures of merit for determination of As(III) using UV-PVG/QT-AAS without and after activation of the apparatus by Bi(III)

	Without activation	After activation
LOD/μg dm^{-3}	89	18
LOQ/μg dm^{-3}	300	60
Sensitivity/dm^3 μg^{-1}	1.1×10^{-4}	1.1×10^{-3}
Repeatability (RSD)/%	1.9	4.5
LDR/μg dm^{-3}	300–1500	60–500

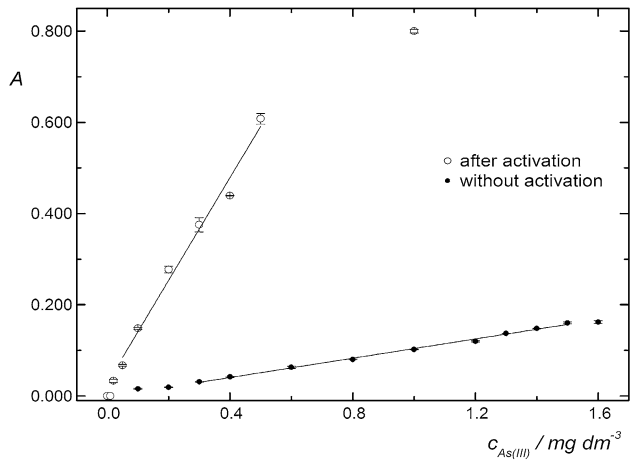

Fig. 5 Calibration dependences of As(III) without and after activation of the apparatus by Bi(III). Used optimum experimental conditions are listed in Table 1

generation technique (UV-PVG) and atomic fluorescence detection [19]. About two orders lower detection limit was achieved for HG-AAS with preconcentration in a cryotrap [17]. It is necessary to mention that AFS is much more sensitive than AAS and cryotrapping can also improve LOD significantly.

On the other hand, no signal was observed for concentration higher than 5 μg dm^{-3} of 2-mercaptoethanol, an organic additive with the highest negative effect of all the studied compounds.

This work shows that UV-photochemical generation of arsenic volatile species is applicable as well as the other techniques of volatile compounds generation. A comparable sensitivity with the other vapour generation techniques, simplicity of the apparatus and an effortless measurement procedure are the advantages of this approach, which is also environmentally friendly.

Moreover, an applicability of this approach for arsenic speciation seems to be possible in future. It was confirmed experimentally that L-cysteine which is often used for sample preparation does not interfere and that acetonitrile (potential mobile phase component) even increase the signal of arsenic in studied concentration range.

Experimental

An analytical method for determination of arsenic using its UV-photochemical volatile compound generation was developed in this work. The arsenic volatile compounds were detected by atomic absorption spectrometer Varian SpectraAA-300A (Varian, Australia) after the atomization in a conventional T-shaped quartz tube (QT-AAS) which was externally heated to 950 °C (RMI, CZ). An arsenic hollow cathode lamp (Heraeus, Germany, current of 10 mA, $\lambda = 193.7$ nm) and a Superlamp (Photron, current of 18 mA, boosted by 20 mA, $\lambda = 193.7$ nm) served as sources of radiation. The used quartz tube atomizer (atomization tube had conventional dimensions) was unique because it had an integrated gas–liquid separator (GLS) with forced outlet at the ending of the inlet arm. The GLS inner volume was approximately 7 cm^3. Both these parts were laboratory-made as one piece of quartz. A scheme of the instrumental set-up for UV-PVG/QT-AAS employed in flow injection mode is depicted in Fig. 6.

Arsenic volatile compounds were generated in a flow-through UV-photoreactor consisting of a 2.5 m-long Teflon (PTFE) tube (1.0 mm ID, 1.4 mm OD) wrapped around a source of UV-radiation. A low-pressure mercury UV bench lamp (254 nm, 20 W, dimensions 610 × 152 × 108 mm) (purchased from Ushio, Japan) was used as the source of UV-radiation.

Formic acid was pumped to the UV-photochemical reactor using a MasterFlex programmable peristaltic pump with an eight-channel Ismatec head (Cole-Parmer, USA). The sample was injected into the flow of carrier liquid by a six-way injection valve via a 600 mm^3 injection loop. Hydrogen was introduced to the apparatus before the UV-photochemical reactor and its flow rate was controlled by a flowmeter (Cole-Parmer, USA, model 32907-67, range 0–1000 cm^3 min^{-1}). A stream of argon was introduced to the apparatus into two different places (before the six-way injection valve and into the gas–liquid separator). A flowmeter (Cole-Parmer, USA, model N112-02) was used for regulation of total argon flow rate. Tygon and Teflon tubes of various inner diameters and lengths were used as a connection material in the apparatus.

Reagents and samples

Deionized water prepared in a $MilliQ_{plus}$ system (18.2 MΩ cm; Millipore, USA) was used for dilution of all the solutions. The stock solution of As(III) was prepared by dissolving the appropriate amount of arsenic trioxide (>99.5 %, Sigma–Aldrich, USA) in slightly alkaline (solid KOH—89.0 %, Lach-Ner, CZ) solution. Formic acid (HCOOH, ≥98 %, Sigma–Aldrich, USA) was used as UV-

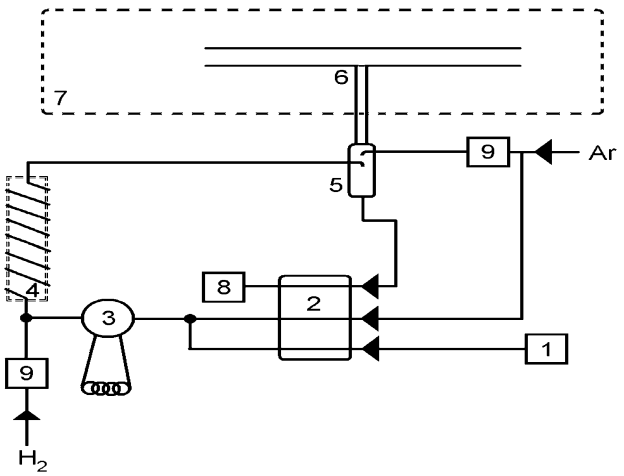

Fig. 6 A scheme of the instrumental set-up for UV-PVG/QT-AAS (FIA). *1* reservoir bottle with solution of HCOOH, *2* peristaltic pump, *3* six-way injection valve, *4* UV-lamp with reaction coil, *5* gas–liquid separator with forced outlet integrated to, *6* externally heated quartz tube atomizer, *7* AAS, *8* waste bottle, *9* gas flow controller

photochemical reaction agent and its solutions were prepared fresh daily. Argon (99.998 %; Linde Gas, CZ) was used as the inert carrier gas during all the experiments. Hydrogen (99.998 %; Linde Gas, CZ) was used as the reaction gas during all the experiments.

The solutions of the studied compounds or ions were prepared from standard solution of Fe(III) (1002 ± 2 mg dm^{-3}, Merck, Germany), Co(II) (1002 ± 2 mg dm^{-3}, Merck, Germany), Ni(II) (1000 ± 5 mg dm^{-3}, Analytika, CZ), Cu(II) (1000 ± 5 mg dm^{-3}, Analytika, CZ), Se(IV) (1000 ± 2 mg dm^{-3}, Analytika, CZ), Bi(III) (1001 ± 5 mg dm^{-3}, Merck, Germany), SO_4^{2-} (1000 ± 2 mg dm^{-3}, Merck, Germany) and Cl^- (1000 ± 2 mg dm^{-3}, Merck, Germany), or diluted from stock solutions of HNO_3 ($\geq$65 %, Merck, Germany), ethanol ($\geq$99.5 %, Merck, Germany), 2-mercaptoethanol ($\geq$99.0 %, Sigma-Aldrich, USA), triethanolamine ($\geq$98 %, Sigma-Aldrich, USA), acetonitrile ($\geq$99.8 %, Sigma-Aldrich, USA) or by dissolving of solid L-cysteine hydrochloride monohydrate ($\geq$98 %, Sigma-Aldrich, USA), TiO_2 ($\geq$99.5 %, size of nanoparticles $\sim$21 nm, Aldrich, USA).

Determination of As(III) by UV-PVG/QT-AAS

Samples prepared in formic acid medium were injected by an injection valve via a 600 mm^3 injection loop into the flow of carrier liquid (a solution of formic acid). Sample zone together with carrier liquid was pumped into the UV-photoreactor where arsenic volatile compounds had been formed under the UV irradiation. The reaction mixture with generated volatile products was transported into a gas–liquid separator. The liquid phase was pumped into the waste while the gaseous phase, which was flushed out by a stream of argon, entered the atomizer.

Acknowledgments The authors acknowledge for financial support from the Charles University in Prague: GAUK152214, Project SVV260317 and Project UNCE204025/2012.

References

1. Marschner K, Musil S, Dědina J (2015) Spectrochim Acta 109:16
2. Rybínová M, Červený V, Hraníček J, Rychlovský P (2015) Microchem J 124:584
3. Sturgeon RE, Mester Z (2002) Appl Spectrosc 56:202
4. Červený V, Rychlovský P, Hraníček J, Šíma J (2009) Chem List 103:652
5. Quadros DPC, Borges DLG (2014) Microchem J 116:244
6. Silva CS, Oreste EQ, Nunes AM, Vieira MA, Ribeiro AS (2012) J Anal At Spectrom 27:689
7. Guo X, Sturgeon RE, Mester Z, Gardner GJ (2003) Anal Chem 75:2092
8. Guo X, Sturgeon RE, Mester Z, Gardner GJ (2003) Appl Organomet Chem 17:575
9. Guo X, Sturgeon RE, Mester Z, Gardner GJ (2003) Environ Sci Technol 37:5645
10. Zheng C, Wu L, Ma Q, Lv Y, Hou X (2008) J Anal At Spectrom 23:514
11. Hou X, Ai X, Jiang X, Deng P, Zheng C, Lv Y (2012) Analyst 137:686
12. Han C, Zheng C, Wang J, Cheng G, Lv Y, Hou X (2007) Anal Bioanal Chem 388:825
13. Zheng C, Sturgeon RE, Hou X (2009) J Anal At Spectrom 24:1452
14. Figueroa R, García M, Lavilla I, Bendicho C (2005) J Spectrochim Acta 60:1556
15. Nóbrega JA, Sturgeon RE, Grinberg P, Gardner GJ, Brophy CS, Garcia EE (2011) J Anal At Spectrom 26:2519
16. Matoušek T, Hernández-Zavala A, Svoboda M, Langrová L, Adair BM, Drobná Z, Thomas DJ, Stýblo M, Dědina J (2008) Spectrochim Acta 63:396
17. Musil S, Matoušek T (2008) Spectrochim Acta 63:685
18. Li H, Luo Y, Li Z, Yang L, Wang Q (2012) Anal Chem 84:2974
19. Zheng C, Ma Q, Wu L, Hou X, Sturgeon RE (2010) Microchem J 95:32
20. Cai Y (2000) Trend Anal Chem 19:62
21. Sun YC, Chang YC, Su CK (2006) Anal Chem 78:2640
22. Shih TT, Hsu IH, Wu JF, Lin CH, Sun YC (2013) J Chromatogr A 1304:101
23. Zheng C, Sturgeon RE, Brophy CS, He S, Hou X (2010) Anal Chem 82:2996
24. Santos EJ, Herrmann AB, Santos AB, Baika LM, Sato CS, Tormen L, Sturgeon RE, Curtius AJ (2010) J Anal At Spectrom 25:1627
25. Guo X, Sturgeon RE, Mester Z, Gardner GJ (2004) Anal Chem 76:2401
26. Sturgeon RE, Willie SN, Mester Z (2006) J Anal At Spectrom 21:263
27. Yin Y, Qiu J, Yang L, Wang Q (2007) Anal Bioanal Chem 388:831
28. Quadros DPC, Campanella B, Onor M, Bramati E, Borges DLG, DÚlivo A (2014) Spectrochim Acta Part B 101:312
29. Šlejkovec Z, Kápolna E, Ipolyi I, Elteren JT (2006) Chemosphere 63:1098

30. Francesconi KA, Kuehnelt D (2004) Analyst 129:373
31. Schaeffer R, Francesconi KA, Kienzl N, Soeroes C, Fodor P, Váradi L, Raml R, Goessler W, Kuehnelt D (2006) Talanta 69:856
32. Guo X, Sturgeon RE, Mester Z, Gardner GJ (2005) J Anal At Spectrom 20:702
33. McSheehy S, Guo X, Sturgeon RE, Mester Z (2005) J Anal At Spectrom 20:709
34. Yin Y, Liu J, He B, Shi J, Jiang G (2009) Microchim Acta 167:289
35. Hesse S, Ristau T, Einax JW (2015) Microchem J 123:42

Spectrochimica Acta Part B 134 (2017) 98–104

Contents lists available at ScienceDirect

Spectrochimica Acta Part B

journal homepage: www.elsevier.com/locate/sab

Analytical note

Flow injection determination of Se in dietary supplements using TiO_2 mediated ultraviolet-photochemical volatile species generation

E. Nováková *, O. Linhart, V. Červený, P. Rychlovský, J. Hraníček

Charles University, Faculty of Science, Department of Analytical Chemistry, Albertov 6, Prague 2 CZ 128 43, Czech Republic

ARTICLE INFO

Article history:
Received 21 February 2017
6 June 2017
Accepted 6 June 2017
Available online 15 June 2017

Keywords:
Dietary supplements
Selenite
Selenate
UV-photochemical volatile species generation

ABSTRACT

This paper proposes a method for determination of selenium content in samples of dietary supplements using TiO_2 mediated UV-photochemical vapor generation with quartz furnace atomic spectrometric detection. The flow-injection method was optimized for determination of selenium in the form of selenite or selenate ions. The limits of detection of the proposed method are 0.89 ng mL^{-1} and 0.68 ng mL^{-1} for selenite and selenate, respectively. Extraction in neutral medium was used for the leaching of selenate and NaOH solution was used for the leaching of selenite. The methods accuracy was verified against the declared amounts of Se in five different samples of over-the-counter dietary supplements and on NIST SRM 3280. The method was also compared to results achieved with determination by electrothermal atomization atomic absorption spectrometry following microwave decomposition. The recovery of selenium during sample preparation was tested by spiking the tablets prior to extraction and estimated to be approximately 100%. An interference study has been carried out to estimate the effect of concomitant elements on the methods accuracy.

1. Introduction

Selenium is an important element with effects on human health. Currently, it is considered an essential trace element but with a very narrow therapeutic range. Se effects on mammals have been re-evaluated several times in the past; it had been considered toxic and carcinogenic until the discovery of selenoamino acids in 1966 [1]. Se is included in human body in proteins with a wide variety of biochemical effects but the cancer protective function is supposed to be caused by Se-containing glutathione peroxidase enzyme decreasing oxidative stress [2]. On the other hand, high doses of Se can cause acute toxic effects and cell apoptosis through the production of reactive oxygen species i.e. through an inverse effect [3]. In addition, Se plays an active role in testosterone synthesis, production of thyroid hormones through iodothyronine deionidase enzyme and is also associated with normal functioning of immune system [4,5]. Chronic Se toxicity in humans results in selenosis, which is characterized by hair loss, nail brittleness, garlic breath, gastrointestinal disturbances, and abnormal functioning of the nervous system [6]. Recent publications also mention an increased risk of type II diabetes associated with increased Se consumption through disruption of insulin signaling cascade [7].

Particularly the possibility that selenium may act as cancer protective agent has led to a widespread marketing of Se containing dietary supplements [8]. However, its complicated behavior in the living organism requires strict control of its consumption. Several studies have tried to determine whether the manufacturer-declared Se contents in dietary supplements can be believed. Some authors lean towards confirming the declared values sometimes with reservations towards the identity of the organic species [8–11]. Other authors raise a warning finger that the real contents may in some cases be different from the manufacturer-declared values [12,13].

Determination of selenium in dietary supplements containing selenized yeast usually requires speciation analysis and is carried out using HPLC separation with atomic fluorescence spectrometric detection (AFS) [14,15] or mass spectrometric detection (MS) [8,16–19]. The determination of total Se content in dietary supplements has so far been determined by electrothermal atomic absorption spectrometry (ETAAS) [9,20], inductively coupled plasma optical emission spectrometry [11] and inductively coupled plasma mass spectrometry [8]. Several works also proposed using chemical hydride generation methods to remove spectral interference from the complicated dietary supplement matrices [10,12,20,21].

Ultraviolet photochemical generation (UV-PVG) is a volatile species generation method based on the use of UV radiation and its application for the determination of Se was pioneered by Guo et al. in 2003 [22–24]. Samples are irradiated dissolved in a low molecular weight organic acid with or without the use of photocatalyst [25,26]. It is known that TiO_2 can catalyze the reduction of selenate to a volatile compound in the presence of formic acid and UV radiation [27–31]. Until now UV-PVG

* Corresponding author.
E-mail address: eliska.novakova@natur.cuni.cz (E. Nováková).

http://dx.doi.org/10.1016/j.sab.2017.06.007
0584-8547/

has been used for the determination of Se in the following samples: seawater [32] and modified seawater samples [33], biological samples [34] and once for the determination of Se(IV) in dietary supplements [35].

Nevertheless, the method published by Rybínová et al. had several drawbacks like being time consuming and requiring complicated sample preparation due to an off-line prereduction of the selenate ion in 6.0 M HCl [35]. This paper presents an improved UV-PVG method utilizing TiO_2 photochemical catalyst and flow injection set up for the determination of Se in samples of dietary supplements. This is the first time that dietary supplements have been analyzed using TiO_2 mediated UV-photochemical generation of volatile Se species. No prereduction of Se(VI) during the sample preparation was necessary. The photochemical catalyst permitted an on-line reduction of Se(VI) during the generation of volatile compounds. The determination has been carried out in flow injection set-up, which reduced the sample consumption and increased the sample throughput.

2. Experimental

2.1. Instrumentation

A schematic diagram of the instrumental set-up is shown in Fig. 1. The flow system consisted of a MasterFlex peristaltic pump (Cole-Parmer, USA) driving the solutions, a low pressure six port injection valve (IDEX, USA) with 200 μL PTFE injection loop, a flow-through UV photoreactor and glass gas-liquid separator (volume 6.2 mL) with forced outlet. A second peristaltic pump (VD ČSAV, Czech Republic) was used to remove the waste solution. The photoreactor consisted of 3.4 m long PTFE tube (i.d. 0.8 mm/o.d. 1.58 mm, Sigma-Aldrich, USA) wrapped around a low pressure mercury UV lamp (253.7 nm, 20 W, dimensions 610 × 152 × 108 mm, USHIO, Japan). The lamp and its reflective housing (Upland, USA) were covered by a lid made from hard cardboard and aluminum foil to protect the analyst from exposure to UV rays. Argon (99.998% purity, Linde, Czech Republic) was introduced into the apparatus prior to the reactor as a carrier gas. Hydrogen (99.90% purity, Linde, Czech Republic) was introduced between the gas-liquid separator and quartz furnace atomizer to facilitate atomization. Digital mass flow controllers for flow rates 1.00–100 mL min^{-1} and 0.50–50 mL min^{-1} (Cole-Parmer, USA) were used to control the flow rates of Ar and H_2 respectively. Tygon tubes of various diameters were used for pumping of solutions, PTFE tubing and PP connecting pieces were used in fluid pathways.

A Solaar 939 AA spectrometer equipped with Se hollow cathode lamp (Heraeus, run at 12 mA) has been used for measurement of atomic absorption. The measurements were carried out at the 196.0 nm line (bandwidth 0.5 nm). Atomization of the evolved volatile products was carried out in an externally heated quartz furnace atomizer (T-shaped, inlet arm length 700 mm, optical arm length 119 mm, internal diameter of the atomizer tube at the position of radical cloud 7.5 mm, RMI, Czech Republic). The atomizer was heated to 950 °C. A combined ultrasonic bath and heater (Elmasonic S, purchased from P-lab, Czech Republic) has been used for the extraction of Se from samples.

Microwave digestion system CEM MDS 2000 (CEM, USA) with pressure sensor was used for total digestion of samples for determination by ETAAS. A HR-CS-AAS ContrAA 700 (Analytik Jena, Germany) equipped with a transversally heated graphite furnace atomizer with integrated platform was used for the determination of Se in samples following total digestion of the samples. The results were used as reference for validation of the proposed method.

2.2. Reagents

Deionized water prepared by the $MilliQ_{Plus}$ system (Millipore, USA) was used throughout the measurements. Formic, acetic and propionic acids (all from Sigma-Aldrich, USA) were tested for the preparation of photochemical reagents; acetic acid (>99.8) diluted to 0.5 mol L^{-1} solution was used in Se determination. TiO_2 suspension (>99.5% purity, nanocrystalline, Sigma-Aldrich, USA) prepared in 0.5 mol L^{-1} acetic acid served as photocatalyst. Selenite and selenate standards with concentration of Se 100 mg L^{-1} were prepared from sodium selenite pentahydrate and sodium selenate decahydrate, respectively (both from Sigma-Aldrich, USA). Sodium hydroxide solution used in extraction was prepared from sodium hydroxide micro pearls (p.a., Lachner, Czech Republic). Standard solutions of Zn(II), Fe(III), Cu(II), Cr(III), Mn(II), Mo(VI), As(III), Sb(III), Ni(II) and Te(IV) prepared in nitric acid (1000 mg L^{-1}, all from Analytika, Czech Republic) were used as stock solutions for interference study. Stock solutions of Ca(II) and Mg(II), were prepared from their nitrate salts and solution of iodide from KI (all from Lachner, Czech Republic). Nitric acid (Merck, Germany) was used for wet digestion of samples. Se stock solution in 2.0% HNO_3 (Analytika, Czech Republic) was used for preparation of calibration standards in ETAAS measurements. All reagents were of analytical or higher purity.

2.3. Composition of samples

Samples were in the form of tablets or capsules. They were denoted A-E, where samples A and D contained Se in the form of sodium selenite and samples B, C and E sodium selenate. The declared Se contents in the analyzed samples ranged from 25 to 55 μg per tablet. We used the

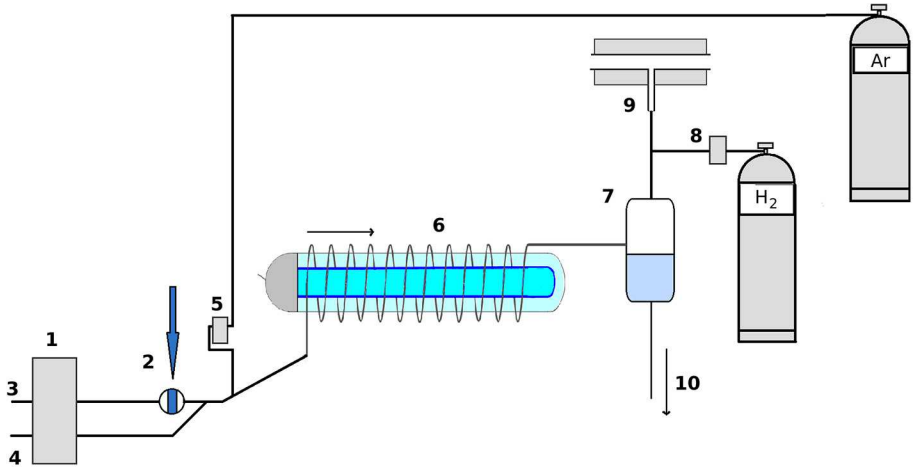

Fig. 1. Experimental set-up for UV-PVG of Se volatile species. 1 – peristaltic pump, 2 – low pressure six-port injection valve, 3 – acetic acid, 4 – photocatalyst suspension, 5 – argon flow rate regulation, 6 – UV-photochemical reactor, 7 – gas liquid separator with forced outlet, 8 – hydrogen flow rate regulation, 9 – externally heated quartz furnace atomizer, 10 – removal of waste solution.

values declared by manufacturers and the contents determined by ETAAS as reference.

NIST SRM 1640a was used for the verification of the accuracy of the UV-photochemical vapor generation. This certified reference material is a semi-synthetic acidified water sample with mass fractions and mass concentrations assigned for 29 elements, 22 of which were gravimetrically added. The solution contains nitric acid at a volume fraction of approximately 2%.

2.4. Preparation of samples of dietary supplements

A suitable extraction method compatible with UV-PVG was necessary to apply the proposed UV-PVG method for the determination of Se in dietary supplements. Use of enzymatic digestion of samples was avoided in order to simplify the extraction procedure. All tablets were weighed and ground to fine powder prior to extraction. The extraction of Se using acetic acid or NaOH was carried out by adding 15 mL of 1.0 mol L^{-1} solution of the selected agent to the weighed aliquots. The sample volume was made up to 50 mL with deionized water. When using extraction at neutral pH the sample was only dispersed in deionized water. The extraction process took 30 min at 35 °C with the help of ultrasound sonication. Subsequently, the samples were filtered through syringe filter with 0.45 μm pore size and polyamide membrane (ProFill PLUS, Fisher Scientific, USA). Filtered samples were diluted 5 or 10 times (sample C during optimization of extraction medium, sample D always) with deionized water.

2.5. CRM samples preparation

The certified reference material SRM 1640a contained nitric acid in concentration sufficient to interfere during UV-PVG [23]; see Section 2.3. Therefore, it was evaporated to near dryness to reduce the nitric acid content. Exactly 40.0 mL of CRM was evaporated and the residue was diluted to 25.0 mL with deionized water. The resulting solution had pH = 2.6.

Due to concerns regarding the complicated sample matrix Se was also determined in NIST SRM 3280 - Multivitamin/Multielement Tablets. To overcome variability between tablets 15 tablets were ground and aliquots were taken to be determined as Se(IV) and Se(VI). Both extraction procedures were used because there was no indication of Se species in the reference material certificate.

2.6. Measurement procedure and evaluation of results

The acid was continuously irradiated by the UV source. Samples were injected into the acid solution and merged with TiO_2 suspension prior to passing through the UV reactor. The signal was recorded for 80 s after sample injection. Peak area was used for quantification in all measurements except for the optimization experiments, where peak height was used instead. The standard deviations in the optimization dependences are based on three successive measurements.

Dietary supplement extracts were determined using both standard addition method and comparison of sample with external calibration. External calibration curves were measured with selenate in deionized water and selenite in the solution of 0.06 mol L^{-1} NaOH to compensate for the effect of NaOH in the sample extracts (corresponds to five times diluted sample). If not stated otherwise, two tablets were analyzed in triplicate and the mean value and SD were calculated from the total of six measurements.

The CRMs and samples used in extraction study were analyzed only by standard addition method. The calibration curve for standard addition was constructed from five points, namely diluted sample and four standard additions. Each point was mean of three replicate measurements; however the mean value and SD of the result (see Table 2 and Section 3.6) correspond to two analyzed tablets.

Interference study was carried out comparing the absorbance of model samples containing 150 ng mL^{-1} Se and a known amount of interferent with reference sample containing only Se. Each solution in the interference study was measured in triplicate.

2.7. Analysis of samples by ETAAS as a reference method

Reference measurement of Se content in the samples was carried out using microwave digestion of samples in HNO_3 and subsequent determination using ETAAS. A tablet was weighed, ground and a sample portion of <0.4 g was transferred to a PTFE digestion vessel with 5.0 ml of concentrated nitric acid. The digestion program was following: 20 min at 40% MW power, 10 min at 80% MW power, 10 min at 100% MW power. Samples were diluted as necessary by 2.0% HNO_3. The temperature program used for the determination of Se by ETAAS was taken from the built-in cookbook of the HR-CS-AAS instrument.

2.8. Evaluation of extraction

Se recovery from the matrix was tested on two selected samples (B, D) with different species and Se content. The aim was to determine whether the sample matrix does not limit the dissolution of Se through adsorption. A tablet was weighed, ground, divided in halves and one half from each ground tablet was analyzed without spiking while the other ground tablet was spiked by standard solution prior to extraction. The additions corresponded to 33 μg of Se in the form of sodium selenate solution (sample B) or 55 μg of Se in the form of sodium selenite solution (sample D).

3. Results and discussion

3.1. Photochemical reagent and irradiation conditions

The optimization of all reaction conditions was carried out with 200 ng mL^{-1} aqueous solutions of selenite and selenate. The optimized parameters were: type and concentration of organic acid, flow rate of organic acid, concentration of TiO_2 and flow rates of Ar and H_2. The atomization temperature was set to 950 °C, which is sufficient for atomization of binary hydrides or alkylated derivatives of hydride forming elements.

Formic, acetic and propionic acids were tested as potential reagents in the concentration range 0.1–2.0 mol L^{-1} using a 3.4 m long reaction tube, total acid flow rate 3.8 mL min^{-1}, TiO_2 concentration 0.005% (m/V) and carrier gas flow rate 20.0 mL min^{-1}. Acetic acid gave higher signals than the other two acids at these conditions for the whole concentration range; the selected optimum concentration of acetic acid was 0.5 mol L^{-1} (see Fig. 2). Formic acid is generally recommended for photochemical generation of volatile selenium species in combination with TiO_2 photocatalyst [30,36–39], although acetic [31] or propionic acid can be used too [40]. To our knowledge, no studies compared the performance of TiO_2 mediated UV-PVG in formic and acetic acid yet. In non-catalyzed PVG some insight into the problem of optimum acid choice was recently published by Campanella et al. [41], who studied the effect of temperature on UV-photochemical vapor generation of volatile Se species. They found out that the use of formic acid resulted in higher sensitivity compared to acetic acid when the sample solution was preheated prior to entering the reactor while the signals achieved with acetic acid did not show temperature dependence in the range 25–50 °C.

We found during optimization of the reaction coil length that 3.4 m long reactor is sufficient corresponding to residence time of 34 s. Total acetic acid flow rate 3.0 mL min^{-1} was selected as optimum for this length of reaction coil. TiO_2 prepared in the form of suspension in the diluted organic was added downstream of the injection port; its flow rate was not optimized separately from the flow rate of acid. The ratio of TiO_2 suspension flow rate to acid flow rate was 1:3 and the flow rates given

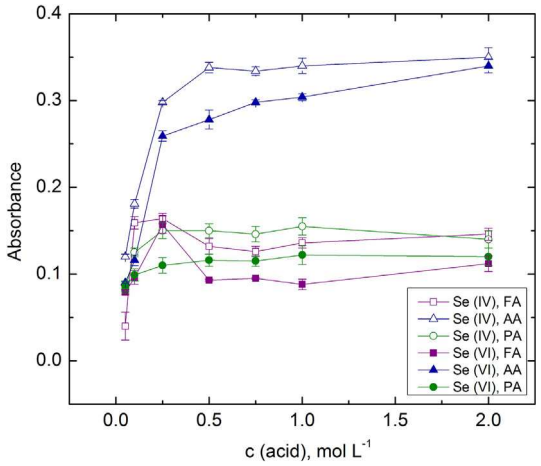

Fig. 2. Effect of type and concentration of organic acid on the sensitivity of TiO_2 mediated UV-photochemical vapor generation, 200 ng mL^{-1} Se(IV) and Se(VI), FA- formic acid, AA – acetic acid, PA – propionic acid, $n = 3$.

are total. Optimization of the TiO_2 suspension concentration over two orders of magnitude yielded highest responses of both species at the original concentration 0.005% (m/V). For the dependences of the signal on the acetic acid flow rate, the concentration of TiO_2 suspension, reaction coil length see Figs. S1–S3 (Appendix, Section S1), respectively.

3.2. Flow rates of gasses

Increasing the flow rate of Ar carrier gas led to the increase of response, however flow rates exceeding 50 mL min^{-1} led to the introduction of condensed phase from the gas liquid separator into the atomizer inlet thus increasing the standard deviation of measurements. The effect was more pronounced for Se(VI) than for Se(IV). Flow rate of 55 mL min^{-1} was selected as a compromise between the sensitivity and the repeatability of measurements. For the dependence of the signal on carrier gas flow rate see Fig. S4 (Appendix, Section S1). Flow rate of H_2 did not have pronounced effect in the region of 2.0–10.0 mL min^{-1} in concordance with the finding that it is necessary only in amount required for successful atomization of the generated volatile compound [42]. Flow rate of 4.2 mL min^{-1} was selected for further measurements.

3.3. Injected volume

The optimization of injection volume was carried out in the range of 30–500 μL. The increase of response was linear; injection volume of 200 μL was selected as it offered good sensitivity while producing symmetrical peaks suitable for integration and determination of Se from both peak height and area.

3.4. Figures of merit

Figures of merit for both Se oxidation states were determined in deionized water and selenite was also determined in 0.06 mol L^{-1} NaOH solution (see Section 2.6 for explanation). We observed that the addition of NaOH to the analyte solution did not affect the figures of merit of the method. Table 1 shows that the figures of merit for both species are comparable. The limits of detection (LOD) and quantification (LOQ) were calculated according to the IUPAC recommendations. The resulting values represent the concentration corresponding to a signal equal to three and ten times, of the standard deviation of ten repeated measurements of Se solution with a concentration below the expected LOD values; solutions containing 0.3 ng mL^{-1} of Se species were used. The LOQ defines the lower end of the linear dynamic range (LDR). The repeatability expressed as the relative standard deviation (% RSD, $n = 10$) was determined at the concentration of 125 ng mL^{-1} of the respective Se species. The sample throughput was 46 analyses per hour. The limits of detection and experimental procedures have also been compared to other published methods on the determination of Se in dietary supplements (see Table 2). The proposed method offers advantageous simplicity compared to some of the published procedures while retaining sufficiently low LOD values. These are in some cases comparable with the use of more sensitive detection techniques like AFS.

Table 1
Figures of merit of TiO_2 mediated UV-photochemical generation of Se species.

	Se(IV)[a]	Se(IV)[b]	Se(VI)[a]
LOD, ng mL^{-1}	0.79	0.89	0.68
Sensitivity, mL ng^{-1} s^{-1}	0.050	0.052	0.048
RSD, %[c]	3.1	1.5	3.3
LDR, ng mL^{-1}	3–250	3–250	2–250

[a] Determined in deionized water.
[b] Determined in 0.06 mol L^{-1} NaOH solution.
[c] Based on 10 replicate measurements of 125 ng mL^{-1} solution.

3.5. Extraction method and determined Se content

Extraction approaches using deionized water and different concentrations of acetic acid and sodium hydroxide [45] were tested and compared to find suitable pH for leaching of Se. Acidic extraction did not yield satisfactory results. Values below the declared content were found in all cases, possibly due to the amount of dissolved interfering species or low extraction efficiency. Sodium selenite could be quantitatively extracted by 0.3 mol L^{-1} NaOH and sodium selenate by water. The achieved results are shown in Table 3. The results obtained using the external calibration method and the standard addition method were compared using a paired *t*-test and no statistically significant difference was found. The results achieved using external calibration method corresponded better with the manufacturer declared values and also with the values found using MW digestion and ETAAS determination. Large standard deviations between samples were observed using both proposed UV-photochemical generation method and ETAAS (see Table 3). Notably smaller deviation was observed when analyzing the certified reference material (see Section 3.6) leading to the conclusion that this effect is associated with the matrix of the dietary supplements samples. Analysis of SRM 3280 showed that when the sample consists of a mix of more tablets the repeatability is improved. It would seem that despite the automated production process there is some variability between the tablets.

3.6. Accuracy assessment

The accuracy of the UV-photochemical vapor generation was tested by analyzing the NIST SRM 1640a certified reference material. The found value 20 ± 1 ng mL^{-1} was in good agreement with the declared value 20.13 ± 0.17 ng mL^{-1}. It is necessary to note that this approach tested only the accuracy of the vapor generation method used. The whole method was validated by determination of Se in SRM 3280. The material was processed as Se(IV) and Se(VI) as no indication regarding the nature of Se species was given. The results were 17.3 ± 0.2 μg g^{-1} (as selenite) and 17.5 ± 0.7 μg g^{-1} and therefore in good agreement with the certified value 17.42 ± 0.45 μg g^{-1}. The recovery of Se from the dietary supplement matrix was validated by carrying out experiments with spiked and non-spiked samples B and D (see Section 2.8). The recoveries counted from the difference between spiked and non-spiked samples were 107 ± 14% for sample B and 104 ± 9% for sample D. The results show that the added selenium was not adsorbed on the solid sample matrix during the sonication and filtration. The overall accuracy of the Se determination in dietary supplements was further demonstrated by the agreement of values found by the proposed and established (ETAAS) method.

Table 2
Comparison of achieved LODs and experimental procedures with other published methods dealing with the determination of Se in dietary supplements.

Method	LOD	Details	
FI-TiO_2/UV–PVG-AAS	0.89 ng mL^{-1} for Se(IV), 0.68 ng mL^{-1} for Se(VI)	30 min extraction, sample throughput 46 runs per hour, no prereduction of Se(VI)	This work
FI-HG-AFS	0.4 ng mL^{-1}	Microwave digestion, only Se(IV), sample throughput 50 samples/h	[21]
HPLC-MS	38–860 pg mL^{-1} for Se(IV)[a], 28–590 pg mL^{-1} for Se(VI)[a]	Reversed phase and ion-pair chromatography, Se(IV), Se(VI), Se-cystine, Se-methionine, Se-ethionine	[43]
ETAAS	0.18 μg g^{-1}	Microwave digestion of samples in HNO_3/H_2O_2, total determination of Se content	[20]
HG-AAS	0.06 μg g^{-1}	Microwave digestion of sample followed by evaporation to dryness, prereduction of Se(VI) in HCl at 95 °C, 15 min	[20]
LC-HG-UV-AFS	0.40 ng mL^{-1} for Se(IV)[b], 1.7 ng mL^{-1} for Se(VI)[b]	Se(IV), Se(VI), Se-methionine, Se-cystine, UV assisted cracking for reduction of Se(VI)	[15]
USAED-HPLC-ETAAS	437 ng g^{-1} for Se(IV), 764 ng g^{-1} for Se(VI)	Ultrasonic assisted enzymatic digestion, coupling of HPLC and ETAAS	[9]
Total reflection XRF	0.1–0.2 mg kg^{-1} of Se[c]	Solid sample analysis, total determination of Se content	[44]
HPLC-HG-AAS	10 ng mL^{-1} for both Se(IV) and Se(VI)	Separation of inorganic Se species, on-line reduction of Se(VI)	[12]
HG-HSSPME-MWP-OES	3.2 ng mL^{-1}	Alkaline dissolution using TMAH, headspace SPME for preconcentration of the generated Se hydride, only Se(IV)	[11]
RP-HPLC-ICPMS	0.06 ng mL^{-1} for Se(IV), 0.07 ng mL^{-1} for Se(VI)	Extraction using acidic mobile phase and protease XIV, Se(IV), Se(VI), Se-methionine, Se-methyl-Se-cysteine, Se-cystine	[17]
UV-PVG-AAS	0.04 ng L^{-1} for Se(IV)	Reduction of Se(VI) at 90–95 °C for 60 min, sample throughput 18 samples/h	[35]

[a] Depending on HPLC separation mode and nebuliser used.
[b] The detection limits were calculated on the basis of 3σ (σ being the residual standard deviation around the regression line) using the regression lines for the standards.
[c] LODs calculated for two different samples.

3.7. Interference study

Interference study was carried out with 50 ng mL^{-1} of Se species in the sample. The interferents were element species present in more than one of the selected dietary supplements, namely Ca(II), Mg(II), Zn(II), Fe(III), Cu(II), Cr(III), Mn(II), Mo(VI) and I(-I) in concentration ranges corresponding to the interferent-to-Se ratio content declared in the dietary supplements. Experiments were also carried out with elements, which are not approved for dietary supplements, but are likely to seriously affect UV-PVG of Se [22,39,41]: As(III), Sb(III), Ni(II), Te(IV). The recoveries are summarized in Table 4. The interference study was carried out in deionized water for Se(VI) and 0.06 mol L^{-1} NaOH for Se(IV).

The presence of interferents manifested itself by deformation of the peak signal. In general, interferences would be more pronounced when evaluating peak height than peak area. Samples without interferent were introduced randomly into the measurement sequence to determine whether the concomitants caused memory effects. No such behavior was observed, probably due to utilizing a flow injection mode of analysis.

Of the tested elements Mn (II), Cr(III) and Mo(VI) did not cause notable interference in either medium at the given concentrations. The negative effect of transition metals was more pronounced for Se(IV) in the presence of 0.06 mol L^{-1} sodium hydroxide than for Se(VI) in deionized water. A possible explanation lies in the formation of precipitates as Zn(II), Fe(III), Ni(II) and Cu(II) are capable of forming poorly soluble compounds with NaOH [46]. These precipitates may adsorb either the analytes or the reaction intermediates; the adsorption of selenite is known for ferric oxyhydroxides [47]. Nevertheless, it is likely that during analysis of real samples these elements were retained in the precipitate during filtering and therefore did not interfere in the determination of Se. Unlike the extracts of the real samples the solutions used in the interference study were not filtered. The small amount precipitate which formed in some cases has been left to settle on the bottom of the volumetric flask and the analysis was carried out on the solution above it. Although the spiking of samples proved that Se is not adsorbed on the matrix, we cannot rule out that possibility if Se is in contact with the interferent for longer time than 30 min. Ca(II) and Mg (II) decreased the repeatability of analytical signals without species and pH preference and Mg(II) increased the signal for Se(IV). This finding is noteworthy as these elements are abundant in dietary supplement samples. On the contrary, presence of Sb(III), As(III) and Te(IV) affected Se(VI) more than Se(IV). In spite of expecting decreased analytical signals due to competition with the other hydride forming elements, the presence of Te(IV) led to 40% increase of Se(VI) response.

Table 3
Determination of Se content in samples of dietary supplements.

Sample	Standard addition method, μg	External calibration method, μg	MW digestion ETAAS, μg	Declared content, μg
A[a]	51 ± 4	52 ± 3	49 ± 4	50
B[b]	36 ± 2	34 ± 3	33 ± 4	30
C[b]	61 ± 9	59 ± 6	51 ± 3	55
D[a]	57 ± 2	55 ± 2	53 ± 5	55
E[b]	22 ± 5	24 ± 2	26 ± 6	25

For detailed information see Section 2.6.
[a] Samples contained sodium selenite and were extracted using NaOH.
[b] Samples contained sodium selenate and were extracted using deionized water.

Table 4
Influence of the selected possible interferents on the recovery of 150 ng mL^{-1} of Se(IV) and Se(VI).

	Interferent concentration	Se(IV) recovery (%) [a]	Se(VI) recovery (%) [b]
Mn(II)	4 mg L^{-1}	97 ± 1	98 ± 3
Zn(II)	1 mg L^{-1}	77 ± 2	97 ± 2
	10 mg L^{-1}	74 ± 6	95 ± 5
Fe(III)	15 mg L^{-1}	85 ± 1	100 ± 4
Cu(II)	500 μg L^{-1}	60 ± 4	93 ± 5
Cr(III)	100 μg L^{-1}	93 ± 5	103 ± 5
Mo(VI)	50 μg L^{-1}	100 ± 2	109 ± 5
I(-I)	150 μg L^{-1}	105 ± 4	105 ± 9
Mg(II)	100 mg L^{-1}	139 ± 9	112 ± 10
Ca(II)	100 mg L^{-1}	103 ± 2	110 ± 3
	200 mg L^{-1}	113 ± 15	115 ± 19
Sb(III)	100 μg L^{-1}	96 ± 6	95 ± 5
	5 mg L^{-1}	86 ± 10	64 ± 8
As(III)	100 μg L^{-1}	94 ± 3	94 ± 2
	5 mg L^{-1}	107 ± 2	78 ± 4
Te(IV)	500 μg L^{-1}	100 ± 2	139 ± 1
	5 mg L^{-1}	98 ± 1	141 ± 1
Ni(II)	5 mg L^{-1}	75 ± 1	101 ± 3
	10 mg L^{-1}	72 ± 1	97 ± 1

$n = 3$.
[a] Determined in 0.06 mol L^{-1} NaOH solution.
[b] Determined in deionized water.

4. Conclusions

A photocatalyst mediated UV-photochemical generation of volatile Se species was successfully demonstrated for the determination of selenite and selenate content in five samples of dietary supplements. Diluted acetic acid was used in combination with TiO_2 as a generation medium. The limits of detection of the method were 0.89 ng mL^{-1} and 0.68 ng mL^{-1} for selenite and selenate, respectively. In determining the total Se content the method was found comparable to using wet microwave digestion and ETAAS determination of Se, while using much simpler procedure. The method proposed in our work is environmentally friendly and permits an easy implementation of automation due to being based on flow injection set-up. Large standard deviations were observed in both the proposed method and ETAAS, which we attributed to the variability of matrix and Se content between the samples.

Acknowledgements

The work was supported by the Charles University (Project SVV260440 and Project GA UK No. 228214). The authors would also like to thank to Jiří Dědina from the Czech Academy of Science for valuable comments.

Appendix A. Supplementary data

Supplementary data to this article can be found online at http://dx.doi.org/10.1016/j.sab.2017.06.007.

References

[1] B. Markert, S. Fränzle, S. Wünschmann, Chemical Evolution - The Biological System of the Elements, Springer, 2015http://dx.doi.org/10.1007/978-3-319-14355-2.
[2] M.P. Rayman, Selenium and human health, Lancet 379 (2012) 1256–1268, http://dx.doi.org/10.1016/S0140-6736(11)61452-9.
[3] M.P. Rayman, Food-chain selenium and human health: emphasis on intake, Br. J. Nutr. 100 (2008) 254–268, http://dx.doi.org/10.1017/S0007114508939830.
[4] M.P. Rayman, The importance of selenium to human health, Lancet 356 (2000) 233–241, http://dx.doi.org/10.1016/S0140-6736(00)02490-9.
[5] L.V. Papp, J. Lu, A. Holmgren, K.K. Khanna, From selenium to selenoproteins: synthesis, identity, and their role in human health, Antioxid. Redox Signal. 9 (2007) 775–806, http://dx.doi.org/10.1089/ars.2007.1528.
[6] M. Navarro-Alarcon, C. Cabrera-Vique, Selenium in food and the human body: a review, Sci. Total Environ. 400 (2008) 115–141, http://dx.doi.org/10.1016/j.scitotenv.2008.06.024.
[7] H. Steinbrenner, B. Speckmann, A. Pinto, H. Sies, High selenium intake and increased diabetes risk: experimental evidence for interplay between selenium and carbohydrate metabolism, J. Clin. Biochem. Nutr. 48 (2010) 40–45, http://dx.doi.org/10.3164/jcbn.11-002FR.
[8] C. B'Hymer, J.A. Caruso, Evaluation of yeast-based selenium food supplements using high-performance liquid chromatography and inductively coupled plasma mass spectrometry, J. Anal. At. Spectrom. 15 (2000) 1531–1539, http://dx.doi.org/10.1039/b006437h.
[9] G. Vale, A. Rodrigues, A. Rocha, R. Rial, A.M. Mota, M.L. Goncalves, L.P. Fonseca, J.L. Capelo, Ultrasonic assisted enzymatic digestion (USAED) coupled with high performance liquid chromatography and electrothermal atomic absorption spectrometry as a powerful tool for total selenium and selenium species control in Se-enriched food supplements, Food Chem. 121 (2010) 268–274, http://dx.doi.org/10.1016/j.foodchem.2009.11.084.
[10] V. Stibilj, P. Smrkolj, A. Krbavčič, Investigation of the declared value of selenium in food supplements by HG-AFS, Microchim. Acta 150 (2005) 323–327, http://dx.doi.org/10.1007/s00604-005-0335-6.
[11] A. Tyburska, K. Jankowski, Determination of selenium in dietary supplements by optical emission spectrometry after alkaline dissolution and subsequent headspace solid phase microextraction, J. Pharm. Biomed. Anal. 74 (2013) 268–272, http://dx.doi.org/10.1016/j.jpba.2012.11.011.
[12] L. Kozak, M. Rudnicka, P. Niedzielski, Determination of inorganic selenium species in dietary supplements by hyphenated analytical system HPLC-HG-AAS, Food Anal. Methods 5 (2012) 1237–1243, http://dx.doi.org/10.1007/s12161-012-9365-y.
[13] P. Niedzielski, M. Rudnicka, M. Wachelka, L. Kozak, M. Rzany, M. Wozniak, Z. Kaskow, Selenium species in selenium fortified dietary supplements, Food Chem. 190 (2016) 454–459, http://dx.doi.org/10.1016/j.foodchem.2015.05.125.
[14] E. Dumont, K. De Cremer, M. Van Hulle, C.C. Chery, F. Vanhaecke, R. Cornelis, Separation and detection of Se-compounds by ion pairing liquid chromatography-microwave assisted hydride generation-atomic fluorescence spectrometry, J. Anal. At. Spectrom. 19 (2004) 167–171, http://dx.doi.org/10.1039/b307316e.
[15] P. Viñas, I. López-García, B. Merino-Meroño, N. Campillo, M. Hernández-Córdoba, Determination of selenium species in infant formulas and dietetic supplements using liquid chromatography-hydride generation atomic fluorescence spectrometry, Anal. Chim. Acta 535 (2005) 49–56, http://dx.doi.org/10.1016/j.aca.2004.11.068.
[16] F. Gosetti, P. Frascarolo, S. Polati, C. Medana, V. Gianotti, P. Palma, R. Aigotti, C. Baiocchi, M.C. Gennaro, Speciation of selenium in diet supplements by HPLC-MS/MS methods, Food Chem. 105 (2007) 1738–1747, http://dx.doi.org/10.1016/j.foodchem.2007.04.072.
[17] Y.-J. Hsieh, S.-J. Jiang, Determination of selenium compounds in food supplements using reversed-phase liquid chromatography–inductively coupled plasma mass spectrometry, Microchem. J. 110 (2013) 1–7, http://dx.doi.org/10.1016/j.microc.2013.01.009.
[18] J. Zembrzuska, H. Matusiewicz, H. Polkowska-Motrenko, E. Chajduk, Simultaneous quantitation and identification of organic and inorganic selenium in diet supplements by liquid chromatography with tandem mass spectrometry, Food Chem. 142 (2014) 178–187, http://dx.doi.org/10.1016/j.foodchem.2013.05.004.
[19] H. Goenaga Infante, G. O'Connor, Ma. Rayman, R. Wahlen, J. Entwisle, P. Norris, R. Hearn, T. Catterick, Selenium speciation analysis of selenium-enriched supplements by HPLC with ultrasonic nebulisation of ICP-MS and electrospray MS/MS detection, J. Anal. At. Spectrom. 19 (2004) 1529–1538, http://dx.doi.org/10.1039/b411270a.
[20] L. Valiente, M. Piccinna, E. Romero Ale, A. Grillo, P. Smichowski, Determination of selenium in dietary supplements by ETAAS and HG-AAS: a comparative study, At. Spectrosc. 23 (2002) 129–134.
[21] L. Gámiz-Gracia, M.D. Luque De Castro, Determination of selenium in nutritional supplements and shampoos by flow injection-hydride generation-atomic fluorescence spectrometry, Talanta 50 (1999) 875–880, http://dx.doi.org/10.1016/S0039-9140(99)00171-X.
[22] X. Guo, R.E. Sturgeon, Z. Mester, G.J. Gardner, UV vapor generation for determination of selenium by heated quartz tube atomic absorption spectrometry, Anal. Chem. 75 (2003) 2092–2099, http://dx.doi.org/10.1021/ac020695h.
[23] X. Guo, R.E. Sturgeon, Z. Mester, G.J. Gardner, Photochemical alkylation of inorganic selenium in the presence of low molecular weight organic acids, Environ. Sci. Technol. 37 (2003) 5645–5650, http://dx.doi.org/10.1021/es034418j.
[24] X. Guo, R.E. Sturgeon, Z. Mester, G.J. Gardner, UV light-mediated alkylation of inorganic selenium, Appl. Organomet. Chem. 17 (2003) 575–579, http://dx.doi.org/10.1002/aoc.473.
[25] Y. Yin, J. Liu, G. Jiang, Photo-induced chemical-vapor generation for sample introduction in atomic spectrometry, TrAC Trends Anal. Chem. 30 (2011) 1672–1684, http://dx.doi.org/10.1016/j.trac.2011.04.021.
[26] Y. He, X. Hou, C. Zheng, R.E. Sturgeon, Critical evaluation of the application of photochemical vapor generation in analytical atomic spectrometry, Anal. Bioanal. Chem. 388 (2007) 769–774, http://dx.doi.org/10.1007/s00216-006-1044-7.
[27] V.N.H. Nguyen, D. Beydoun, R. Amal, Photocatalytic reduction of selenite and selenate using TiO2 photocatalyst, J. Photochem. Photobiol. A Chem. 171 (2005) 113–120, http://dx.doi.org/10.1016/j.jphotochem.2004.09.015.
[28] E. Kikuchi, H. Sakamoto, Kinetics of the reduction reaction of selenate ions by TiO2 photocatalyst, J. Electrochem. Soc. 147 (2000) 4589–4593, http://dx.doi.org/10.1149/1.1394106.
[29] T.T.Y. Tan, D. Beydoun, R. Amal, Photocatalytic reduction of Se (VI) in aqueous solutions in UV/TiO2 system: kinetic modeling and reaction mechanism, J. Phys. Chem. B 107 (2003) 4296–4303, http://dx.doi.org/10.1021/jp026149+.
[30] T. Tan, D. Beydoun, R. Amal, Effects of organic hole scavengers on the photocatalytic reduction of selenium anions, J. Photochem. Photobiol. A Chem. 159 (2003) 273–280, http://dx.doi.org/10.1016/S1010-6030(03)00171-0.
[31] T. Suzuki, R.E. Sturgeon, C. Zheng, A. Hioki, T. Nakazato, H. Tao, Influence of speciation on the response from selenium to UV-photochemical vapor generation, Anal. Sci. 28 (2012) 807–811, http://dx.doi.org/10.2116/analsci.28.807.
[32] M. Garcıá, R. Figueroa, I. Lavilla, C. Bendicho, On-line photoassisted vapour generation implemented in an automated flow-injection/stopped-flow manifold coupled to an atomic detector for determination of selenium, J. Anal. At. Spectrom. 21 (2006) 582–587, http://dx.doi.org/10.1039/b601650b.
[33] R. Figueroa, M. García, I. Lavilla, C. Bendicho, Photoassisted vapor generation in the presence of organic acids for ultrasensitive determination of Se by electrothermal-atomic absorption spectrometry following headspace single-drop microextraction, Spectrochim. Acta B At. Spectrosc. 60 (2005) 1556–1563, http://dx.doi.org/10.1016/j.sab.2005.10.009.
[34] C. Zheng, L. Yang, R.E. Sturgeon, X. Hou, UV photochemical vapor generation sample introduction for determination of Ni, Fe , and Se in biological tissue by isotope dilution ICPMS, Anal. Chem. 82 (2010) 3899–3904, http://dx.doi.org/10.1021/ac1004376.
[35] M. Rybínová, V. Červený, J. Hraníček, P. Rychlovský, UV-photochemical vapor generation with quartz furnace atomic absorption spectrometry for simple and sensitive determination of selenium in dietary supplements, Microchem. J. 124 (2016) 584–593, http://dx.doi.org/10.1016/j.microc.2015.10.004.
[36] Q. Wang, J. Liang, J. Qiu, B. Huang, Online pre-reduction of selenium(VI) with a newly designed UV/TiO2 photocatalysis reduction device, J. Anal. At. Spectrom. 19 (2004) 715–716, http://dx.doi.org/10.1039/b403129f.
[37] Y.C. Sun, Y.C. Chang, C.K. Su, On-line HPLC-UV/Nano-TiO2-ICPMS system for the determination of inorganic selenium species, Anal. Chem. 78 (2006) 2640–2645, http://dx.doi.org/10.1021/ac051899b.
[38] H. Li, Y. Luo, Z. Li, L. Yang, Q. Wang, Nanosemiconductor-based photocatalytic vapor generation systems for subsequent selenium determination and speciation with atomic fluorescence spectrometry and inductively coupled plasma mass spectrometry, Anal. Chem. 84 (2012) 2974–2981, http://dx.doi.org/10.1021/ac3001995.
[39] W. Yang, Y. Gao, L. Wu, X. Hou, C. Zheng, X. Zhu, Preconcentration and in-situ photoreduction of trace selenium using TiO2 nanoparticles, followed by its determination by slurry photochemical vapor generation atomic fluorescence spectrometry,

Microchim. Acta 181 (2014) 197–204, http://dx.doi.org/10.1007/s00604-013-1101-9.
[40] C. Zheng, L. Wu, Q. Ma, Y. Lv, X. Hou, Temperature and nano-TiO2 controlled photochemical vapor generation for inorganic selenium speciation analysis by AFS or ICP-MS without chromatographic separation, J. Anal. At. Spectrom. 23 (2008) 514–520, http://dx.doi.org/10.1039/b713651j.
[41] B. Campanella, A. Menciassi, M. Onor, C. Ferrari, E. Bramanti, A. D'Ulivo, Studies on photochemical vapor generation of selenium with germicidal low power ultraviolet mercury lamp, Spectrochim. Acta B At. Spectrosc. 126 (2016) 11–16, http://dx.doi.org/10.1016/j.sab.2016.10.007.
[42] J. Dědina, B. Welz, Quartz tube atomizers for hydride generation atomic absorption spectrometry: mechanism for atomization of arsine, J. Anal. At. Spectrom. 7 (1992) 307–314, http://dx.doi.org/10.1039/JA9920700307.
[43] J.M. Marchante-Gayón, C. Thomas, I. Feldmann, N. Jakubowski, Comparison of different nebulisers and chromatographic techniques for the speciation of selenium in nutritional commercial supplements by hexapole collision and reaction cell ICP-MS, J. Anal. At. Spectrom. 15 (2000) 1093–1102, http://dx.doi.org/10.1039/b002372h.
[44] H. Stosnach, Analytical determination of selenium in medical samples, staple food and dietary supplements by means of total reflection X-ray fluorescence spectroscopy, Spectrochim. Acta B At. Spectrosc. 65 (2010) 859–863, http://dx.doi.org/10.1016/j.sab.2010.07.001.
[45] L.S. Balistrieri, T. Chao, Adsorption of selenium by amorphous iron oxyhydroxide and manganese dioxide, Geochim. Cosmochim. Acta 54 (1990) 739–751, http://dx.doi.org/10.1016/0016-7037(90)90369-V.
[46] H. Remy, Lehrbuch der anorganischen Chemie, Bd. 2, Akademische Verlagsgesellschaft Geest & Portig K.-G., Leipzig, 1973.
[47] S. Tam, A. Chow, D. Hadley, Effects of organic component on the immobilization of selenium on iron oxyhydroxide, Sci. Total Environ. 164 (1995) 1–7, http://dx.doi.org/10.1016/0048-9697(95)04423-X.

Mercury Speciation in Fish by High-Performance Liquid Chromatography (HPLC) and Post-Column Ultraviolet (UV)-Photochemical Vapor Generation (PVG): Comparison of Conventional Line-Source and High-Resolution Continuum Source (HR-CS) Atomic Absorption Spectrometry (AAS)

Ondřej Linhart[*1], Alžběta Kolorosová-Mrázová[1], Jan Kratzer[2], Jakub Hraníček[1], Václav Červený[1]

[1]Charles University, Faculty of Science, Department of Analytical Chemistry, Albertov 6, CZ-128 43 Prague 2, Czech Republic.
[2]The Czech Academy of Sciences, Institute of Analytical Chemistry, Veveří 97, CZ-602 00 Brno, Czech Republic.
[*]Corresponding author: Ondřej Linhart, Department of Analytical Chemistry, Hlavova 2030/8, CZ-128 43 Prague 2, Czech Republic; e-mail: ondrej.linhart@natur.cuni.cz; telephone number: +420 221 951 220

Abstract

An ultraviolet-photochemical generator (UV-PVG) capable of post-column on-line transformation of both organic and inorganic mercury species to cold vapor (Hg^0) with subsequent detection by quartz tube - atomic absorption spectrometry (QT-AAS) was developed. Mercury(II), methylmercury(I), ethylmercury(I), and phenylmercury(I) were successfully detected after separation by reversed-phase high-performance liquid chromatography (RP-HPLC).. Two types of AAS detectors were compared. The first one was a commonly used line-source instrument while the second was a high-resolution continuum source (HR-CS) AAS. The latter one was found better reaching limits of detection 0.47 μg L^{-1} for Hg(II), 0.84 μg L^{-1} for methylmercury(I), 0.80 μg L^{-1} for ethylmercury(I) and 2.0 μg L^{-1} for phenylmercury(I). The repeatability at 30 μg L^{-1} was 3.6 %, 4.1 %, 6.2 % and 4.5 % for respective species (n=10). These characteristics can compete with those reported for even more sensitive atomic fluorescence spectrometry.

Nine various sample extraction procedures were investigated. Extraction by tetramethylammonium hydroxide and HCl at 75 °C was chosen as the only one compatible with the proposed separation and detection steps reaching high extraction efficiency and no changes in mercury speciation information. Applicability of the proposed method (high-performance liquid chromatography - ultraviolet-photochemical vapor generation - quartz tube - atomic absorption spectrometry) was demonstrated on fish samples and certified reference materials (CRM) DOLT-4 (dogfish liver) and ERM-CE464 (tuna fish). The results were comparable to those obtained by a reference method based on L-cysteine extraction and high-performance liquid chromatography - inductively coupled plasma - mass spectrometry (HPLC-ICP-MS) determination.

Keywords: mercury speciation, high-performance liquid chromatography (HPLC), ultraviolet (UV)-photochemical vapor generation (PVG), and high-resolution continuum source (HR-CS) atomic absorption spectrometry (HR-CS AAS)

Introduction

Mercury is among all heavy metals a pollutant of special concern due to its major impact on human health and the environment. Although all the mercury species are toxic, organic mercury compounds are generally more toxic than inorganic, i.e. mercurous (Hg(I)) and mercuric (Hg(II)) state. The most common organomercurial compounds are methylmercury(I), ethylmercury(I) and phenylmercury(I) (Yin et al. 2007a; Yin et al. 2009; Yin et al. 2007b). The main pathways for human exposure are the consumption of contaminated fish, through dental amalgams, and also through occupational exposure (Cornelis et al. 2005). Since chemical form of mercury controls its bioavailability, transport, persistence and impact on the human body, emphasis is put on speciation analysis of mercury in last years rather than on a simple determination of total mercury content. Thus, a number of analytical techniques have been developed and validated for mercury speciation analysis as reviewed recently (Leopold et al. 2010; Clough et al. 2014).

Methods for mercury speciation can be classified into two general approaches: chromatographic methods including gas chromatography, liquid chromatography, and capillary electrophoresis and non-chromatographic methods based on the different physico-chemical properties of Hg species, i.e. their solubility, volatility, or redox potential (Leopold et al. 2010). Spectrometric detectors such as atomic absorption (AAS), atomic emission (AES), and atomic fluorescence spectrometry (AFS) as well as inductively coupled plasma - mass spectrometry (ICP-MS) can be used as element specific detectors. Chromatographic approaches enable to separate and determine all mercury species of interest in a single step. On the contrary, non-chromatographic approaches mostly determine only one species rather than allowing the simultaneous determination of all present Hg species. The non-chromatographic approaches might be a valuable analytical tool because they are usually less expensive and sophisticated than the set-ups employing chromatography. They could serve as fast screening methods (saving time and money) indicating which samples fulfil the criteria and which should undergo detailed speciation analysis.

Generation of volatile species (VSG) is a useful analytical strategy that can be employed in both non-chromatographic as well as chromatographic methods of speciation analysis. In case of chromatographic method, the VSG is introduced as a post-column derivatization step in order to enhance analyte introduction efficiency into the detector. In principle, there are three different approaches to VSG based on chemical, electrochemical or photochemical reactions.

Chemical generation of volatile species (C-VSG) is realized by $NaBH_4$, $LiAlH_4$ or $SnCl_2$ which require daily preparation of their solutions due to limited stability.

The analyte reduction is performed by electric current in presence of very pure mineral acid in electrochemical VSG (Ec-VSG). Although the need for chemical reductant is eliminated, the electrode passivation or memory effects could affect the determination (Červený et al. 2009).

Photochemical VSG (UV-VSG) employs ultraviolet irradiation of the liquid sample in the photochemical generator which usually consists of a UV-transparent tube realized by quartz (Mo et al. 2017) or thin Teflon tube wrapped around a mercury ultraviolet lamp (Rybínová et al. 2015; Rybínová et al. 2016; Huang et al. 2013). The first work in this field has been reported by Zheng et al. 2005. The UV-VSG is based on analyte reaction with radicals which are formed after ultraviolet irradiation of low molecular weight organic acids such as formic, acetic, etc. (Yin et al. 2007c; Sturgeon 2017; Yin et al. 2007b; Zheng and Hintelmann 2010; Bendl et al. 2006). The formic acid as the strongest carboxylic acid facilitates also sample disintegration (López-Rouco et al. 2008).

In the particular case of Hg speciation analysis, generation of cold mercury vapor (CVG) might be employed as a post-column derivatization step prior to spectrometric detection. A conversion of both inorganic and organomercurial compounds to Hg(0) needs a preliminary step consisting of full oxidation of all the mercury to Hg(II) in C-VSG. Ec-VSG lacks the universality towards mercury species.

The interface for ultraviolet-photochemical vapor generation (UV-PVG) is able to perform the transformation of all organomercurial species to inorganic Hg(II) and then the reduction of Hg(II) to volatile Hg(0) in one step, but only in presence of additional photochemical reagents. The most common one is 2-mercaptoethanol. According to the literature (dos Santos et al. 2010), the optimum formic acid concentration for UV-PVG is 10%. Several other papers (Yin et al. 2007a) discuss the use of TiO_2 as a photo-catalyst improving the performance of the generator, but the results are ambiguous (Sturgeon and Luong 2013). It can be stated that the presence of TiO_2 is not necessary for the UV-photochemical generation of mercury (Yin et al. 2007a; Nováková et al 2017) and its presence does not improve the limit of detection (Han et al. 2007). UV-PVG is a very convenient technique for speciation analysis of mercury by high-performance liquid chromatography with on-line atomic absorption spectrometry detection. This approach has been already successfully tested for determination of phenylmercury(I), ethylmercury(I), methylmercury(I) and Hg(II) (Yin et al. 2008; da Silva et al. 2012).

The extraction of mercury species from sample matrix is mostly based on complex formation (Rydberg et al. 2004), often employing L-cysteine as a complexing agent. Such extractions can be ultrasound-assisted (de Souza et al. 2013) or occur at elevated temperature (Hight and Cheng 2006). In other studies, 2-mercaptoethanol was successfully applied as a complexing agent in combination with microwave extraction (Chang et al. 2007; Leng et al. 2013). López et al. reported ultrasound and enzyme-assisted extraction of Hg species by 2-mercaptoethanol (López et al. 2010). Sodium pyrrolidinedithiocarbamate was used as a complexing agent for extraction of mercury from natural waters (Falter and Schöler 1995). The alkaline digestion method was applied to the samples of marine origin (Yin et al. 2009) and sediments (Ramalhosa et al. 2001). Other possible extraction methods employed nitric and hydrochloric acids in combination with sonication or microwave radiation (Rahman and Kingston 2004). Various extraction methods employing tetramethylammonium hydroxide, KOH in methanol, HCl and a mixture of KBr with $CuSO_4$ have been compared for Hg species extraction (Yun et al. 2013; Gao and Liu 2011). Other studies dealt also with tetramethylammonium hydroxide in combination with microwave radiation and high-performance liquid chromatography - inductively coupled plasma - mass spectrometry detection (Vidler et al. 2007) as well as the capillary gas chromatography - atomic fluorescence spectrometry via pyrolysis (Nevado et al. 2005). A summary of methods employed for mercury speciation analysis with spectrometric detection and their limits of detection is presented in Table 1.

The aim of this work was to develop, optimize and validate on-line coupling of UV-photochemical generation with a preceding reversed-phase high-performance liquid chromatography separation and with detection by quartz tube - atomic absorption spectrometry (QT-AAS). Two types of atomic absorption spectrometers have been tested as detectors. The first was a commonly used line-source instrument while the second was a high-resolution continuum source atomic absorption spectrometer (HR-CS-AAS). To the best of our knowledge, the latter one has never been reported in the literature for on-line speciation analysis of mercury.

Experimental

Standards and reagents

Deionized water from a Milli Q^{plus} system (Millipore, USA) was used for preparation of all solutions. Stock/standard solutions of mercury species (1 $g \cdot L^{-1}$ Hg) were prepared by dissolving of an appropriate amount of solid methylmercury chloride (MeHgCl, Sigma-Aldrich, Germany), ethylmercury chloride (EtHgCl, Supelco, Germany), and phenylmercury chloride (PhHgCl, Supelco, Germany) in 40% (v/v) ethanol (Merck, Germany). On the contrary, mercury chloride ($HgCl_2$, Sigma-Aldrich, Germany) was dissolved in deionized water. All standard solutions were stored in a fridge at 5 °C. All working solutions were prepared daily prior analysis by dilution in mobile phase.

The mobile phase consisted of three components: (i) an organic solvent, (ii) buffer system, and (iii) photochemical reagent. Two types of buffer systems were tested: acetic acid and ammonium or sodium acetate (both analytical grade, Sigma-Aldrich, Germany). Methanol (Fluka, Germany), acetonitrile (Sigma-Aldrich, Germany), and ethanol (Merck, Germany) were examined as organic solvents. 2-mercaptoethanol (≥99%, Sigma-Aldrich, Germany) was employed as the photochemical reagent. Argon (99.998%, Linde Gas, Czech Republic) served as carrier a gas.

Tetramethylammonium hydroxide (25% (v/v), Sigma-Aldrich, USA), HCl (37%, Merck, Germany), KOH (Lach-Ner, Czech Republic), dichloromethane (≥99.8%, Sigma-Aldrich, USA), $CuSO_4$ (Biogema, Slovak Republic), KBr (Sigma-Aldrich, USA), H_2SO_4 (Merck, Germany), L-cysteine.HCl (≥98%, Sigma-Aldrich, USA), L-cysteine (for biochemistry, Merck, Germany), sodium pyrrolidinedithiocarbamate (Sigma-Aldrich, USA) and thioglycolic acid (Merck, Germany) were used for mercury species extraction.

Real samples

The fishes examined were collected from the Pastviny river dam on Divoká Orlice river in the Czech Republic. Two different fish species were selected for analysis: muscle tissue of a chub *(Leuciscus cephalus)* and muscle tissue of a zander (*Sander lucioperca*). A certified reference materials ERM-CE464 (tuna fish, Sigma-Aldrich, Germany) and DOLT-4 (dogfish liver, National Research Council of Canada, Canada) were employed to assess the accuracy (trueness and precision) of the results.

Instrumentation

The high-performance liquid chromatography setups as well as atomic absorption spectrometry detectors were different for (i) optimization study of generation and separation steps and (ii) method validation as well as measurement of real samples under optimized conditions. Both experimental setups employed are described below. Moreover, the results of the determination of the mercury species in the real samples (fish tissue and certified reference materials (CRM)) found by the proposed high-performance liquid chromatography - ultraviolet-photochemical vapor generation - quartz tube atomic absorption spectrometry method were compared to those obtained by reference measurements by advanced mercury analyzer (AMA 254) (total Hg content determination) and high-performance liquid chromatography - inductively coupled plasma - mass spectrometry (reference speciation analysis method).

Experimental setup for the optimization study

A diagram of the instrumental set-up for high-performance liquid chromatography - ultraviolet-photochemical vapor generation - quartz tube - atomic absorption spectrometry is shown in Fig. 1.

The cold mercury vapor was generated in the ultraviolet-photochemical generator consisting of the ultraviolet radiation source, low-pressure Hg vapor ultraviolet-lamp (20 W, 253.7 nm, Ushio, Japan) with a Teflon tube (1 m long, 1 mm i.d., 2 mm o.d.) reaction coil wrapped around it. The ultraviolet-lamp was supplied by a power source (Modus SB 118; Czech Republic). Argon as a carrier gas was introduced into the apparatus upstream the ultraviolet-photochemical reactor. The cold mercury vapor was transported to the gas-liquid separator (GLS) with forced outlet. The cold mercury vapor was detected by a line-source atomic absorption spectrometer Varian (Varian SpetrAA-300A, Australia). The mercury hollow cathode lamp (Varian, Australia) operated at 253.7 nm with spectral bandwidth of 0.5 nm and a lamp current 4 mA. The AAS was equipped with a quartz detection tube (QT) with integrated gas-liquid separator having inner volume of 9 mL. The inlet arm of laboratory made T-shaped quartz tube was externally heated to 150 °C by resistance wire to eliminate water vapor condensation and analyte losses. The dimensions of quartz tube were as follows: the length of optical arm was 120 mm (14 mm i.d.) with narrow middle part (50 mm in length, 7 mm i.d.) and the length of connecting tube between quartz tube and gas-liquid separator was 70 mm (6

mm i.d.). The liquid phase from gas-liquid separator was drained out to the waste by a peristaltic pump Masterflex® (Cole-Parmer, USA).

An ultra high-performance liquid chromatography RS 3000 system (Dionex, USA) with an autosampler equipped with 100 μL sample loop and a Gemini column (C18, 110 Å, 3 μm, 150 mm length, 2.4 mm i.d., Phenomenex, USA) were employed. This column is termed short column in further text since another Gemini C18 column was tested in this work which was longer and broader (see below).

Experimental setup for method validation and real sample measurements

The same ultra high-performance liquid chromatography system and autosampler were used, but the column was replaced by another Gemini separation column (C18, 110 Å, 3 μm, 250 mm length, 3 mm i.d., Phenomenex, USA) termed long column further in the text. This long column was combined with a guard column (C18, 3.2 x 8 mm, 3 μm, Phenomenex, USA) to protect it. A high-resolution continuum source atomic absorption spectrometer ContrAA700 (Analytik Jena, Germany) was used as a detector. Measurements were performed at 253.6519 nm line selected from the continuous spectrum of Xe lamp of the instrument with data collection of 3 pixels (center pixel ± 1) of the charge-coupled device detector using high-performance liquid chromatography mode of the control software.

Determination of total mercury content

Total mercury content was determined without any sample pretreatment employing advanced mercury analyzer (AMA 254) produced by Altec, Czech Republic. This single purpose atomic absorption spectrometer is based on in situ dry ashing of the sample at ca 750 °C in the stream of oxygen followed by amalgamation of Hg on gold surface with subsequent detection by atomic absorption spectrometry. About 5-100 mg of the frozen tissue or untreated reference material was weighed into the nickel sample boat and the analysis was performed using following parameters: drying period of 60 s and decomposition period of 200 s. Peak height of the transient signals was evaluated by the software of the spectrometer.

Reference method for Hg speciation analysis

Speciation analysis of mercury by high-performance liquid chromatography - inductively coupled plasma - mass spectrometry (HPLC-ICP-MS) was performed using the

conditions described in an Agilent application note (Sannac and Chen 2012). An isocratic HPLC pump (Agilent 1200) and an Agilent HPLC autosampler (model 1260 Infinity with 20 μL loop) were used to drive the mobile phase and inject the filtered samples onto an Agilent Zorbax Eclipse XDB-C18 column (4.6 x 150 mm, 5 μm). A guard column (Agilent Zorbax Eclipse XDB-C18, 4.6 x 12.5 mm, 5 μm) was employed to protect the separation column. The mobile phase was pumped at a flow rate of 1 mL min^{-1} and consisted of 0.5 g L^{-1} of L-cysteine hydrochloride monohydrate and 0.5 g L^{-1} of L-cysteine both dissolved in deionized water (pH adjusted to 2.3 by HCl addition) with 2% methanol. An Agilent 7700x ICP-MS spectrometer was used as a detector. Mercury isotopes ^{201}Hg and ^{202}Hg were monitored. An internal standard (250 ng mL^{-1} Te) was co-nebulized to monitor the plasma conditions employing ^{125}Te isotope. The chromatogram signals were evaluated in an Agilent Mass Hunter Workstation software (version B.01.01).

Extraction – reference method

Extraction of mercury species from the fish tissue samples as well as reference materials was performed by a procedure slightly modified from that reported previously (Hight and Cheng 2006). A dry thermostat (model LT-200, Hach-Lange, Germany) was employed for extraction of the mercury species. About 100 mg of reference material or the frozen sample was weighed into the glass vials of the thermostat and 5 mL of 0.2 % aqueous solution of L-cysteine hydrochloride monohydrate was added. Vials were capped tightly, shaken vigorously by hand and subsequently let to heat to 60 °C for 2 hours. The vials were shaken by hand every 30 minutes during heating. After that the vials were cooled down to room temperature for 15 minutes and the content from the vials was quantitatively transferred into 10 mL volumetric flasks and diluted by deionized water. The samples were filtered subsequently through 0.45 μm PTFE membrane filters (Hach-Lange, Germany).

Extraction methods tested

Based on the literature search (see the chapter *Introduction*), several promising extraction agents and techniques were selected as summarized in Table 2. At first, all nine extraction methods and extraction agents were tested in flow injection analysis mode to protect separation column and save time. The sample weight of 200 mg was always employed. The sample extracts were always centrifuged in a benchtop centrifuge (Chirana, Czech Republic)

and subsequently filtered through a syringe filter with 47 mm diameter (regenerated cellulose, pore size 0.45 μm, Whatman, UK) prior measurement.

Only one of the extraction methods tested (extraction with tetramethylammonium hydroxide and HCl at 75 °C for 30 minutes, row 9 in Table 2) was found compatible with the proposed high-performance liquid chromatography - ultraviolet-photochemical vapor generation - quartz tube - atomic absorption spectrometry method. All the other extraction agents or procedures were found incompatible due to significant suppression of Hg species signals or changes in speciation information.

Extraction with tetramethylammonium hydroxide and HCl at 75 °C

About 200 mg of the frozen sample or reference material was weighed and 6 mL of extraction agent was added. The concentration of tetramethylammonium hydroxide was 6.25% (w/v) and of HCl 0.05 mol L^{-1}. The extraction was carried out on a heating mantle LTHS 500 (ETA, Czech Republic) under a reflux condenser at approximately 75 °C for 30 minutes. This extraction procedure was chosen as the best and was used for the next experiments with fish tissues and certified reference materials.

Proposed method and measurement procedure

The mobile phase consisted of sodium acetate buffer system (equimolar mixture of 20 mmol L^{-1} CH_3COOH and CH_3COONa, pH 4.75), 2-mercaptoethanol (0.1%) as a photochemical reagent and ethanol (40% v/v) as an organic solvent. The sample volume of 100 μL was injected into the stream of mobile phase. The mercury species were separated on the column. Carrier gas (Ar) at a flow rate of 100 mL min^{-1} was introduced to the system through a T-junction between separation column and UV-photochemical reactor. All mercury species were subsequently eluted to the UV-photochemical generator in which they were decomposed to the mercuric ion (Hg(II)) and immediately after that reduced to cold mercury vapor Hg(0). The mixture of liquid and gaseous phase was transported by a flow of the carrier gas and mobile phase into the gas-liquid separator. The evaporated mercury was transported consequently by an Ar stream to the externally heated quartz tube (150 °C) to be detected by AAS. The liquid phase was pumped to the waste. The distance between the UV-photochemical reactor, gas-liquid separator and the quartz detection tube was kept as short as possible.

Results and discussion

Two crucial steps of the proposed method, namely high-performance liquid chromatography separation of Hg species and their subsequent conversion to Hg vapor in an ultraviolet-photochemical generator (UV-PVG), were optimized. Firstly, the key experimental conditions of the UV-PVG were optimized in a flow injection mode. These parameters were: the construction of UV-photochemical reactor, the carrier liquid composition as well as its flow rate and carrier gas flow rate.

Since the UV-photochemical generator was used as a post-column derivatization unit for speciation analysis, separation of mercury species by reversed-phase high-performance liquid chromatography was optimized in the next part of this work. Following key parameters were optimized in this step: the mobile phase composition, its pH and flow rate, column temperature and flow rate of Ar.

All experimental parameters were subsequently optimized again in the high-performance liquid chromatography mode and the compromised conditions for both steps were chosen to achieve the best results.

Optimization of the UV-photochemical generation of mercury vapor

Reaction coil

One of the essential parameters of any UV-photochemical reactor is the construction of its reaction coil. The material and wall thickness affect the transparency for radiation from the ultraviolet lamp which intensity obviously influences the UV-PVG efficiency. The length of reaction coil affects the irradiation time which is very important for transformation of Hg(II) and organic species into Hg(0). Therefore, Teflon (PTFE) tubes with different inner (i.d.) and outer (o.d.) diameters (0.8 mm i.d./1.6 mm o.d.; 1.0 mm i.d./2.0 mm o.d.; 0.5 mm i.d./1.5 mm o.d.) and lengths (from 0.5 to 5 m) were tested in this work. All experiments were performed in flow injection analysis mode with standards of Hg(II), methylmercury(I) and ethylmercury(I) at 500 μg L^{-1} concentration levels. A 100 cm long PTFE tube with 1.0 mm i.d./2.0 mm o.d. was selected as the most suitable reaction coil for all the further measurements.

Carrier gas flow rate

The carrier gas (Ar) flow rate and way of its introduction to the system (up- or downstream the UV-photochemical generator) have an impact on sensitivity and total time of measurement. The results have shown the same trend for all mercury species tested. With increasing the gas flow rate from 30 to 100 mL min^{-1} the peak became higher and narrower resulting in higher sample throughput and shorter measurement time. Flow rates between 100 and 200 mL min^{-1} Ar resulted in signal decrease owning to higher dilution of mercury vapor in detection tube and/or lower generation efficiency because of shorter irradiation time. For next experiments, the Ar flow rate of 100 mL min^{-1} was selected as optimum with gas introduction upstream the UV-photochemical reactor.

Composition of carrier liquid

The signal of mercury species could be also affected by composition of the carrier liquid and concentration of its components. Moreover, in the particular case of high-performance liquid chromatography coupling to UV-PVG, the carrier liquid serves also as a mobile phase. Thus, its composition affects both the separation of mercury species as well as subsequent UV-photochemical generation step. The carrier liquid is thus termed mobile phase further in the text. It consists of a buffer system, organic solvent and a photochemical reagent which concentration levels are optimized below.

Acetate buffer composition and concentration

The components of carrier liquid tested in ultraviolet-photochemical vapor generation step were pre-selected with respect to be compatible with the high-performance liquid chromatography separation. Ammonium acetate and sodium acetate were tested employing Hg(II) as a model species in solution with the concentration range of 0-50 mmol L^{-1} in flow injection analysis arrangement. Very low signals were detected when no buffer was present in the mobile phase. Compared to the sodium acetate buffer, ammonium acetate provided lower Hg(II) signals. Further experiments have revealed that buffer concentration did not influence the separation step significantly. Therefore, sodium acetate at concentration 20 mmol L^{-1} was chosen as optimum.

pH of sodium acetate

The effect of mobile phase pH on the UV-photochemical generation was investigated in the range from pH 4.0 to 8.0 employing Hg(II), methylmercury(I) and ethylmercury(I) standard solutions as model species. The maximum absorbance was reached at pH 4.75 for all species tested.

Organic solvents

Methanol, ethanol and acetonitrile were tested firstly just in the ultraviolet-photochemical vapor generation step in flow injection analysis mode for the sake of simplicity without preceding high-performance liquid chromatography separation. Acetonitrile caused significant reduction of absorbance. Although both methanol and ethanol (from 0 to 50 % (v/v)) provided very similar results, ethanol at a concentration of 10 % was selected for further experiments due to higher response of Hg(II).

Photochemical reagent

According to Yin et al. 2009b, the presence of 2-mercaptoethanol is necessary for ultraviolet-photochemical vapor generation from all Hg species. According to our results, only Hg(II) was detected without 2-mercaptoethanol. Its presence was found crucial for ultraviolet-photochemical cold vapor generation from organomercurials. The effect of 2-mercaptoethanol concentration was studied from 0 to 0.2 % (v/v) in flow injection analysis mode. The optimum concentration of 2-mercaptoethanol was 0.1 % (v/v).

Optimum parameters found for the ultraviolet-photochemical cold mercury vapor generation with quartz tube - atomic absorption detection are summarized in Table 3.

Optimization of Hg species separation by high-performance liquid chromatography

Organic solvent

Acetonitrile was found as unsuitable organic solvent since it suppressed signals of mercury species during the UV-PVG as discussed above. An inefficient separation of Hg(II) and methylmercury(I) was observed with methanol. The mobile phase containing ethanol provided better separation even though the two species, Hg(II) and methylmercury(I), were not baseline separated on the short column (150 mm – see *Experimental*). With the increasing

concentration of ethanol from 10 % (v/v) to 40 % (v/v), the signals of all examined mercury species rose and the retention times were shorter. Therefore, 40 % (v/v) ethanol was chosen as the compromise between efficiency of high-performance liquid chromatography separation and efficiency of UV-PVG.

2-mercaptoethanol

According to Yin et al. 2009 and Yin et al. 2007b, the presence of 2-mercaptoethanol was necessary not only for UV-PVG but also for high-performance liquid chromatography separation. Effect of no addition of 2-mercaptoethanol on separation efficiency of the species could not have been tested since the organomercurials would not be subsequently reduced in the UV-reactor as discussed above. For this reason, the effect of 2-mercaptoethanol concentration on high-performance liquid chromatography separation was studied from 0.05 to 0.2 %. The signals of Hg(II), methylmercury(I), ethylmercury(I), and phenylmercury(I) increased with concentration of 2-mercaptoethanol and then decreased slowly. The content of 2-mercaptoethanol of 0.1 % (v/v) was chosen as the best for effective separation and efficient UV-PVG from all Hg species.

Temperature of the column

Influence of column temperature on the separation process was investigated in the range of 23-50 °C. The column temperature played very important role in this method due to the high viscosity of the ethanol:water (40:60) mixture resulting in high back pressure. In accord with the theory, the back pressure of the column was lower with increased column temperature as a consequence of decreased viscosity of the mobile phase. As a result, mobile phase flow rate could be increased up to 1 mL min^{-1} at column temperature of 50 °C. Temperature of 40 °C was selected for the best resolution of Hg(II) and methylmercury(I) peaks.

Mobile phase flow rate

The column backpressure of a mixture of ethanol with aqueous solution of sodium acetate buffer (40 % and 60 %, respectively) at 40 °C at a mobile phase flow rate of 0.50 mL min^{-1} exceeded 245 bars which is the maximum value recommended by the manufacturer. Therefore, only lower flow rates of the mobile phase have been investigated. Peak heights of all mercury species rose with the increasing flow rate of mobile phase. However, peaks of Hg(II) and methylmercury(I) were not separated when the flow rate of mobile phase was higher than 0.30 mL min^{-1}. Consequently, the 0.30 mL min^{-1} mobile phase flow rate was selected as the optimum value.

Optimum experimental conditions

Optimum experimental conditions found in this work for the proposed reversed-phase high-performance liquid chromatography separation and subsequent UV-PVG from all selected Hg species are summarized in Table 4.

Figures of merit

After optimization of both UV-PVG and high-performance liquid chromatography separation, the analytical figures of merit were determined employing longer (250 mm – see *Experimental*) separation column and a high-resolution continuum source atomic absorption spectrometer with the aim to attain better resolution of peaks and higher sensitivity of the determination. The calibration curves of Hg(II), methylmercury(I), ethylmercury(I), and phenylmercury(I) were constructed employing a solution of mixed-species standards with concentration levels ranging from 0 to 100 μg L^{-1} of each mercury species under optimum experimental conditions listed in Table 4. Due to increasing concentration of each mercury compound, the calibration curve was bended towards the axis of concentration above 100 μg L^{-1}. Linear parts of calibrations are displayed in Fig. 2.

The method parameters were calculated from peak area and all figures of merit are summarized in Table 5 for all mercury species under optimum conditions listed in Table 4. Limits of detection and quantitation, respectively were calculated as the concentration giving a response equal to three times (ten times) the standard deviation of peak areas of ten repeated measurements of mixed-species standard solution with a concentration of 2.5 μg L^{-1} of

individual species. Attained limits of detection are comparable to those reported in literature (see Table 1). They can even compete with more sensitive atomic fluorescence detectors.

Fig. 3 shows two chromatograms recorded for the same model mixture of Hg species (50 μg L^{-1} of each species) employing two different apparatus setups: 1) line source AAS as a detector with preceding reversed-phase high-performance liquid chromatography separation on the short (150 mm) column and 2) HR-CS-AAS detector with separation on a long (250 mm) column. The use of long separation column results obviously in better peak resolution since the short column was not capable of baseline-separation of Hg(II) and methylmercury(I) species. The optimization experiments had shown that it was not possible to improve the resolution in other way than changing the column length while maintaining the same separation mechanism. As a consequence, the analysis takes longer since the retention times are shifted to higher values. Both the experimental setups were operated under optimized conditions.

It must be once again highlighted that the improvement in separation depicted in Fig. 3 is not caused by the detector but it is obviously attributed to the length of the column. However, the use of more sensitive as well as more selective HR-CS-AAS detector led to significant improvement in the signal to noise ratio. Unfortunately, the way of signal and data processing differed for both spectrometers significantly. Therefore, it is not possible to easily compare peak heights or peak areas recorded between the two spectrometers but the signal to noise ratio improvement can be clearly seen from Fig. 3. To the best of our knowledge this is the first report on HR-CS-AAS detector employed for on-line speciation analysis of mercury and evaluation of its performance.

Sample analysis

Two fish samples and two certified reference materials were analyzed under the optimum conditions by the proposed reversed-phase high-performance liquid chromatography - ultraviolet-photochemical vapor generation - quartz tube - atomic absorption spectrometry method after extraction by tetramethylammonium hydroxide and HCl at 75 °C for 30 minutes (see Table 2 and *Experimental* for details). The results have been compared to that attained by high-performance liquid chromatography - inductively coupled plasma - mass spectrometry after L-cysteine extraction and AMA 254 which were used as reference methods (see *Experimental* for details).

Analyses of both certified reference materials were performed with good agreement between the certified Hg(II) and methylmercury(I) contents and the experimentally found

Hg(II) and methylmercury(I) contents. The extraction efficiency of mercury (total Hg) was comparable for both, proposed and reference method, reaching 80-90 %. No significant conversions among Hg species were observed for either proposed or reference method. See Table 6 for summary of the results attained during the reversed-phase high-performance liquid chromatography - ultraviolet-photochemical vapor generation - quartz tube - atomic absorption spectrometry method validation.

Conclusions

The ultraviolet (UV)-photochemical generator of mercury cold vapor was constructed and optimized for speciation analysis of mercury compounds. Four selected mercury species (Hg(II), methylmercury(I), ethylmercury(I) and phenylmercury(I)) were individually decomposed and subsequently reduced to mercury cold vapor in the presence of acetic acid, ethanol and 2-mercaptoethanol under the UV-irradiation. Both the acetic acid and 2-mercaptoethanol were found to act as photochemical agents for organomercurials, whereas acetic acid alone is capable of conversion of Hg(II) to Hg(0) only.

Subsequently, reversed-phase high-performance liquid chromatography was connected prior to the UV-photochemical generator developed which served as a derivatization device for atomic absorption spectrometry (AAS) detection. Compromise experimental conditions compatible with both, the separation and UV-photochemical generation, were selected for further use. With the aim to attain better separation efficiency and higher signal to noise ratio, long separation column and high-resolution continuum source (HR-CS) AAS were employed for method characterization and validation. Low limits of detection (ranging from 0.5 to 2 μg L^{-1}), good precision (repeatability lower than 6.2 % relative standard deviation for 10 measurements) and satisfactory separation efficiency were achieved in the developed set-up. These method characteristics are comparable even with values typical for atomic fluorescence spectrometry (AFS) detection which is considered as more sensitive technique.

Based on the literature, nine various extraction agents and procedures were tested and their compatibility with both, reversed-phase high-performance liquid chromatography separation and UV-photochemical generation, was investigated. The extraction mixtures tested include: HCl and ethanol; 2-mercaptoethanol; thioglycolic acid; sodium pyrrolidinedithiocarbamate; KOH in methanol; L-cysteine; KBr and $CuSO_4$ and a mixture of tetramethylammonium hydroxide/HCl. The last combination of tetramethylammonium hydroxide and HCl at 75 °C was chosen as the best and the only one suitable with respect to high extraction efficiency of mercury species and no changes in mercury speciation information.

The applicability of the proposed procedure comprising of Hg species extraction followed by reversed-phase high-performance liquid chromatography separation and post-column UV-photochemical vapor generation (UV-PVG) derivatization with subsequent AAS detection was demonstrated on Hg speciation analysis in fish samples and certified reference

materials of tuna fish (ERM-CE464) and dogfish liver (DOLT-4) with a similar matrix. The results were comparable to those obtained with a reference method based on L-cysteine extraction and high-performance liquid chromatography - inductively coupled plasma - mass spectrometry (HPLC-ICP-MS) separation/detection showing the potential of the developed method.

Acknowledgements. This research has been supported by the Charles University (Project SVV260440, PROGRES Q46, UNCE 204025/2012, OP VaVpI Project EU CZ.02.2.67/0.0/0.0/16_016/0002266, Project GA UK No. 152214) and the Czech Academy of Sciences, Institute of Analytical Chemistry (Institutional Research Plan No. RVO: 68081715).

References

Bendl, R., J. Madden, A. L. Regan, and N. Fitzgerald. 2006. Mercury determination by cold vapor atomic absorption spectrometry utilizing UV photoreduction. Talanta 68: 1366–1370. doi:10.1016/j.talanta.2005.07.061

Chang, L. F., S. J. Jiang, and A. C. Sahayam. 2007. Speciation analysis of mercury and lead in fish samples using liquid chromatography–inductively coupled plasma mass spectrometry. Journal of Chromatography *A* 1176: 143–148. doi:10.1016/j.chroma.2007.10.072

Clough, R., C. F. Harrington, S. J. Hill, Y. Madrid, and J. F. Tyson 2014. Atomic spectrometry updates. Review of advances in elemental speciation. Journal of Analytical Atomic Spectrometry 28: 1153-1195. doi:10.1039/c3ja90039h

Cornelis, R., J. Caruso, H. Crews, and K. Heumann. 2005. Handbook of Elemental Speciation II. John Wiley&Sons Ltd, Chichester.

Červený, V., P. Rychlovský, J. Hraníček, and J. Šíma, 2009. Elektrochemické generování těkavých sloučenin pro potřeby spektrálních analytických metod. Chemické Listy 103: 652–660.

Falter, R., and H. Schöler. 1995. Determination of mercury species in natural waters at picogram level with on-line RP C18 preconcentration and HPLC-UV-PCO-CVAAS. Fresenius Journal of Analytical Chemistry 353: 34–38. doi: doi.org/10.1007/BF00322887

Gao, E., and J. Liu. 2011. Rapid determination of mercury species in sewage sludge by high-performance liquid chromatography on-line coupled with cold-vapor atomic-fluorescence spectrometry after ultrasound-assisted extraction. Analytical Sciences 27: 637–641. doi: doi.org/10.2116/analsci.27.637

Nováková, E., O. Linhart, V. Červený, P. Rychlovský, and J. Hraníček. 2017. Flow injection determination of Se in dietary supplements using TiO_2 mediated ultraviolet-photochemical volatile species generation. Spectrochemica Acta Part B 134: 98-104. doi:10.1016/j.sab.2017.06.007

Han, C., C. Zheng, J. Wang, and G. Cheng. 2007. Photo-induced cold vapor generation with low molecular weight alcohol, aldehyde, or carboxylic acid for atomic fluorescence spectrometric determination of mercury. Analytical and Bioanalytical Chemistry 338: 825–830. doi:10.1007/s00216-006-1006-0

Hight, S. C., and J. Cheng. 2006. Determination of methylmercury and estimation of total mercury in seafood using high performance liquid chromatography (HPLC) and inductively coupled plasma-mass spectrometry (ICP-MS): Method development and validation. Analytical Chimica Acta 567: 160–172. doi:10.1016/j.aca.2006.03.048

Huang, K., K. Xu, X. Hou, Y. Jia, Ch. Zheng and L. Yang. 2013. UV-induced atomization of gaseous mercury hydrides for atomic fluorescence spectrometric detection of inorganic and organic mercury after high performance liquid chromatographic separation. Journal of Analytical Atomic Spectrometry 28: 510-515. doi:10.1039/c3ja30363b

Leng, G., L. Feng, S.B. Li, P. Yang, and D.Z. Dan. 2013. Speciation analysis of mercury in sediments by HPLC using HPLC hyphenated to vapour generation atomic flourescence spectrometry following microwave-assisted extraction. LC GC Europe 26: 250-258.

Leopold, K., M. Foulkes, and P. Worsfold. 2010. Methods for the determination and speciation of mercury in natural waters - A review. Analytica Chimica Acta 663: 127–138. doi:10.1016/j.aca.2010.01.048

López-Rouco, A., E. Stanisz, H. Matusiewicz, I. Lavilla, and C. Bendicho. 2008. UV reduction with ultrasound-assisted gas–liquid separation for the determination of mercury in biotissues by atomic absorption spectrometry. Journal of Analytical Atomic Spectrometry 23: 1026-1029. doi:10.1039/b802612b

López, I., S. Cuello, C. Cámara, and Y. Madrid. 2010. Approach for rapid extraction and speciation of mercury using a microtip ultrasonic probe followed by LC-ICP-MS. Talanta 82: 594–599. doi:10.1016/j.talanta.2010.05.013
Mo, J., Q. Li, X. Guo, G. Zhang, and Z. Wang. 2017. Flow Injection Photochemical Vapor Generation Coupled with Miniaturized Solution-Cathode Glow Discharge Atomic Emission Spectrometry for Determination and Speciation Analysis of Mercury. Analytical Chemistry 89: 10353–10360. doi:10.1021/acs.analchem.7b02214
Nevado, J. J. B., R. C. R. Martín-Doimeadios, F. J. G. Bernardo, and M. J. Moreno. 2005. Determination of mercury species in fish reference materials by gas chromatography-atomic fluorescence detection after closed-vessel microwave-assisted extraction. Journal of Chromatography *A* 1093: 21–28. doi:10.1016/J.CHROMA.2005.07.054
Quadros, D. P. C., B. Campanella, M. Onor, E. Bramanti, D. L. G. Brorges, and A. D´Ulivo. 2014. Mercury speciation by high-performance liquid chromatography atomic fluorescence spectrometry using an integrated microwave/UV interface. Optimization of a single step procedure for the simultaneous photo-oxidation of mercury species and photo-generation of Hg^0. Spectrochimica Acta Part B: Atomic Spectroscopy 101: 312-319. doi:10.1016/j.sab.2014.09.019
Rahman, G. M. M., and H. M. Kingston. 2004. Application of speciated isotope dilution mass spectrometry to evaluate extraction methods for determining mercury speciation in soils and sediments. Analytical Chemistry 76: 3548–3555. doi:10.1021/ac030407x
Ramalhosa, E., S. Río Segade, E. Pereira, C. Vale, and A. Duarte. 2001. Simple methodology for methylmercury and inorganic mercury determinations by high-performance liquid chromatography-cold vapour atomic fluorescence spectrometry. Analytica Chimica Acta 448: 135–143. doi:10.1016/S0003-2670(01)01317-4
Rybínová, M., V. Červený, J. Hraníček, and P. Rychlovský. 2015. UV-fotochemické generování těkavých sloučenin pro potřeby atomových spektrometrických metod. Chemické Listy 109: 930–937
Rybínová, M., S. Musil, V. Červený, M. Vobecký, and P. Rychlovský. 2016. UV-photochemical vapor generation of selenium for atomic absorption spectrometry: Optimization and ^{75}Se radiotracer efficiency study. Spectrochimica Acta Part B: Atomic Spectroscopy 123: 134–142. doi:10.1016/j.sab.2016.08.009
Rydberg, J., C. Cox M, Musikas, and G. Choppin. 2004. Solvent extraction principles and practice. Marcel Dekker, New York
Sannac, S., and Y. Chen. 2012. Benefits of HPLC-ICP-MS coupling for mercury speciation in food. Agilent Technologies, Manchester.
Santos, E. J., A. B. Herrmann, A. B. dos Santos, L. M. Baika, Ch. S. Sato, L. Tormen, R. E. Sturgeon, and A. J. Curtius. 2010. Determination of thimerosal in human and veterinarian vaccines by photochemical vapor generation coupled to ICP OES. Journal of Analytical Atomic Spectrometry 25: 1627-1632. doi:10.1039/c0ja00029a
Silva, C. S., E. Q. Oreste, A. M. Nunes, M. A. Viera, and A. S. Riberio. 2012. Determination of mercury in ethanol biofuel by photochemical vapor generation. Journal of Analytical Atomic Spectrometry 27: 689-694. doi:10.1039/c2ja10281a
Souza, S., A. D. Campiglia, and F. Barbosa. 2013. A simple method for methylmercury, inorganic mercury and ethylmercury determination in plasma samples by high performance liquid chromatography–cold-vapor-inductively coupled plasma mass spectrometry. Analytical Chimica Acta 761: 11–17. doi:10.1016/J.ACA.2012.11.038
Sturgeon, R. E. 2017. Photochemical vapor generation: a radical approach to analyte introduction for atomic spectrometry. Journal of Analytical Atomic Spectrometry 32: 2319-2340. doi:10.1039/C7JA00285H
Sturgeon, R. E., and V. Luong. 2013. Photo- and thermo-chemical vapor generation of mercury.

Journal of Analytical Atomic Spectrometry 28: 1610-1619. doi:10.1039/c3ja50152c
Yin, Y., J. Qiu, L. Yang, Q. and Wang. 2007b. A new vapor generation system for mercury species based on the UV irradiation of mercaptoethanol used in the determination of total and methyl mercury in environmental and biological samples by atomic fluorescence spectrometry. Analytical and Bioanalytical Chemistry 388: 831–836. doi:10.1007/s00216-007-1122-5
Yin, Y., J. Liang, L. Yang, and Q. Wang. 2007a. Vapour generation at a UV/TiO_2 photocatalysis reaction device for determination and speciation of mercury by AFS and HPLC-AFS. Journal of Analytical Atomic Spectrometry 22: 330–334. doi:10.1039/b614555h
Yin, Y., J. Liu, B. He, J. Shi, and G. Jinag. 2009. Mercury speciation by a high performance liquid chromatography-atomic fluorescence spectrometry hyphenated system with photo-induced chemical vapour generation reagent in the mobile phase. Microchimica Acta 167: 289–295. doi:10.1007/s00604-009-0250-3
Yin, Y., J. Liu, B. He, and G. Jiang. 2007c. Photo-induced chemical vapour generation with formic acid: novel interface for high performance liquid chromatography-atomic fluorescence spectrometry hyphenated system and application in speciation of mercury. Journal of Analytical Atomic Spectrometry 22: 822–826. doi:10.1039/b701514c
Yin, Y., J. Liu, B. He, J. Shi, and G. Jiang. 2008. Simple interface of high-performance liquid chromatography–atomic fluorescence spectrometry hyphenated system for speciation of mercury based on photo-induced chemical vapour generation with formic acid in mobile phase as reaction reagent. Journal of Chromatography A 1181: 77–82. doi:10.1016/j.chroma.2007.12.050
Yun, Z., B. He, Z. Wang, T. Wang, and G. Jiang. 2013. Evaluation of different extraction procedures for determination of organic Mercury species in petroleum by high performance liquid chromatography coupled with cold vapor atomic fluorescence spectrometry. Talanta 106: 60–65. doi:10.1016/j.talanta.2012.12.009
Vidler, D. S., R. O. Jenkins, J. F. Hall, and C. F. Harrington. 2007. The determination of methylmercury in biological samples by HPLC coupled to ICP-MS detection. Applied Organometallic Chemistry 21: 303–310. doi:10.1002/aoc.1173
Zheng, Ch., Y. Li, Y. He, Q. Ma, and X. Hou. 2005. Photo-induced chemical vapor generation with formic acid for ultrasensitive atomic fluorescence spectrometric determination of mercury: potential application to mercury speciation in water. Journal of Analytical Atomic Spectrometry 20: 746-750. doi:10.1039/b503727a
Zheng, W., and H. Hintelmann. 2010. Isotope fractionation of mercury during its photochemical reduction by low-molecular-weight organic compounds. Journal of Physical Chemistry A 114: 4246–4253. doi:10.1021/jp9111348

Table 1. Methods for mercury speciation analysis with spectrometric detection and corresponding limits of detection

Generation, separation	Detection	Detection limits (μg L^{-1})				Reference
		Mercury(II)	Methylmercury(I)	Ethylmercury(I)	Phenylmercury(I)	
Ultraviolet /2-mercaptoethanol	Atomic fluorescence spectroscopy	0.06	0.05	-	-	Yin et al. 2007b
High-performance liquid chromatography - ultraviolet-photochemical vapor generation	Atomic fluorescence spectroscopy	0.085	0.033	0.029	0.038	Yin et al. 2008
High-performance liquid chromatography - ultraviolet-photochemical vapor generation	Atomic fluorescence spectroscopy	0.53	0.22	0.18	0.25	Yin et al. 2009
Ultraviolet-photochemical vapor generation	Atomic absorption spectroscopy	0.05	0.08	0.06	-	Silva et al. 2012
High-performance liquid chromatography - ultraviolet-photochemicalvapor generation	Atomic fluorescence spectroscopy	0.38	0.41	0.56	-	Huang et al. 2013
High-performance liquid chromatography - atomic fluorescence spectroscopy using an integrated microwave/ultraviolet interface	Atomic fluorescence spectroscopy	0.15	0.15	0.35	-	Quadros et al. 2014
High-performance liquid chromatography - ultraviolet–	**Quartz tube-high-resolution continuum source -**	**0.47**	**0.84**	**0.80**	**1.96**	**This work**

photochemical vapor generation	**atomic absorption spectrometry**				
	Quartz tube-line-source - atomic absorption spectrometry	**8**	**31**	**16**	**38**

Table 2. Tested extraction methods

	Extraction method	Extraction agent	Reference
1	7 min ultrasonic bath	7.5 mL of 2% (v/v) hydrochloric acid and 10% (v/v) ethanol	Souza et al. 2013
2	8 min microwave extraction 60 W, ambient temperature	3 ml of 0.1% (v/v) 2-mercaptoethanol	Leng et al. 2013
3	3 hours of shaking 45 min. ultrasonic bath, ambient temperature	25% (m/v) KOH in methanol 1.5 mL of HCl and 6 ml dichloromethane was added	Yin et al. 2009b
4	ambient temperature	6.25 g $CuSO_4$ and 4.5 g KBr with 1.25 mL H_2SO_4 in deionized water	Yun et al.2013
5	Heated for 2 hours at 50-60 °C	5 mL of 0.2% (m/v) of L-cysteine	Hight and Cheng 2006
6	Heated for 2 hours at 50-60 °C	0.2% (v/v) solution of 2-mercaptoethanol in 2% (v/v) methanol	Chang et al. 2007
7	Heated for 2 hours at 50-60 °C	5 mL of 0.2% (m/v) of sodium pyrrolidinedithiocarbamate	Falter and Schöler 1995
8	Microwave extraction 60 W, 25 min	2 mL of 6.25% tetramethylammonium hydroxide 0.05 mol L^{-1} HCl	Vidler et al. 2007
9	Extraction at 75 °C, 30 min	2 mL of 6.25% tetramethylammonium hydroxide 0.05 mol L^{-1} HCl	Zheng and Hintelmann 2010

Table 3. Optimum experimental conditions for UV-photochemical generation of mercury species

Parameter	Experimental conditions
PTFE reaction coil dimensions/(cm)	100 x 0.1 i.d. x 0.2 o.d.
Carrier gas flow rate/(mL min^{-1} Ar)	100
Mobile phase flow rate/(mL min^{-1})	2.5
Sample injection volume/(μL)	200
Concentration of buffer CH_3COOH/CH_3COONa/(mmol L^{-1})	20/20
Buffer pH	4.75
Concentration of 2-mercaptoethanol (v/v)/(%)	0.1
Concentration of ethanol (v/v)/(%)	10

Table 4: Optimum experimental conditions for the proposed method, separation on a long column and detection by high-resolution continuum-source atomic absorption spectrometry.

Parameter	Optimum value
Flow rate of mobile phase/(mL min^{-1})	0.3
Sample injection/(μL)	50
Carrier gas flow rate/(mL min^{-1})	100
Temperature of the column/(°C)	40
Temperature of detection tube/(°C)	150
Reaction coil/(cm)	100 x 0.1 i.d. x 0.2 o.d.
Ethanol content (v/v)/(%)	40
2-mercaptoethanol content (v/v)/(%)	0.1
Concentration of buffer	20/20
CH_3COOH/CH_3COONa/(mmol L^{-1})	
Buffer pH	4.75

Table 5. Analytical figures of merit for the proposed method, separation on a long column and detection by high-resolution continuum-source atomic absorption spectrometry.

Parameter	Mercury(II)	Methylmercury(I)	Ethylmercury(I)	Phenylmercury(I)
Limit of detection/(μg L^{-1})	0.47	0.84	0.80	2.0
Limit of quantitation /(μg L^{-1})	1.6	2.8	2.7	6.5
Sensitivity/(L μg^{-1})	0.10	0.051	0.059	0.053
Repeatability/(% of relative standard deviation at 30 μg L^{-1}; n=10)	3.6	4.1	6.2	4.5
Linear dynamic range up to/(μg L^{-1})	100	100	100	100
Correlation coefficient	0.999	0.998	0.999	0.999

Table 6. Comparison of the results reached by the proposed and reference methods. Mercury speciation analysis in certified reference materials and fish samples. Each value was calculated from three repetitions.

Sample	Species	Certified (mg kg^{-1})	High-performance liquid chromatography - ultraviolet-photochemical vapor generation - quartz tube-atomic absorption spectrometry (mg kg^{-1})	High-performance liquid chromatography - inductively coupled plasma - mass spectrometry (mg kg^{-1})	Total Hg analysis by advanced mercury analyzer (mg kg^{-1})	Extraction efficiency* (%)
DOLT-4 (dogfish liver)	Mercury(II)	1.25[#]	1.16 ± 0.03	1.14 ± 0.04		93/91
	Methylmercury(I)	1.33 ± 0.12	0.96 ± 0.03	1.08 ± 0.01		72/81
	Total Hg	2.58 ± 0.22	2.12 ± 0.04	2.23 ± 0.05	2.53 ± 0.15	82/88
ERM-CE464 (tuna fish)	Mercury(II)	-	0.72 ± 0.08	0.15 ± 0.01	-	
	Methylmercury(I)	5.50 ± 0.17	3.63 ± 0.19	4.08 ± 0.05	-	66/74
	Total Hg	5.24 ± 0.10	4.35 ± 0.21	4.24 ± 0.06	5.03 ± 0.21	86/84
Chub - muscle	Mercury(II)	-	0.22 ± 0.01	< limit of quantitation	-	
	Methylmercury(I)	-	0.41 ± 0.002	0.56 ± 0.02	-	
	Total Hg	-	0.63 ± 0.01	0.56 ± 0.02	0.71 ± 0.02	89/79
Zander - muscle	Mercury(II)	-	0.05 ± 0.01	< limit of quantitation	-	
	Methylmercury(I)	-	0.98 ±0.03	1.12 ± 0.02	-	
	Total Hg	-	1.02 ± 0.03	1.12 ± 0.02	1.30 ± 0.08	79/86

[*] extraction efficiency found by the proposed method/reference methods related to the certified or calculated value

[#] calculated value (difference of certified values: Total Hg - Methylmercury(I))

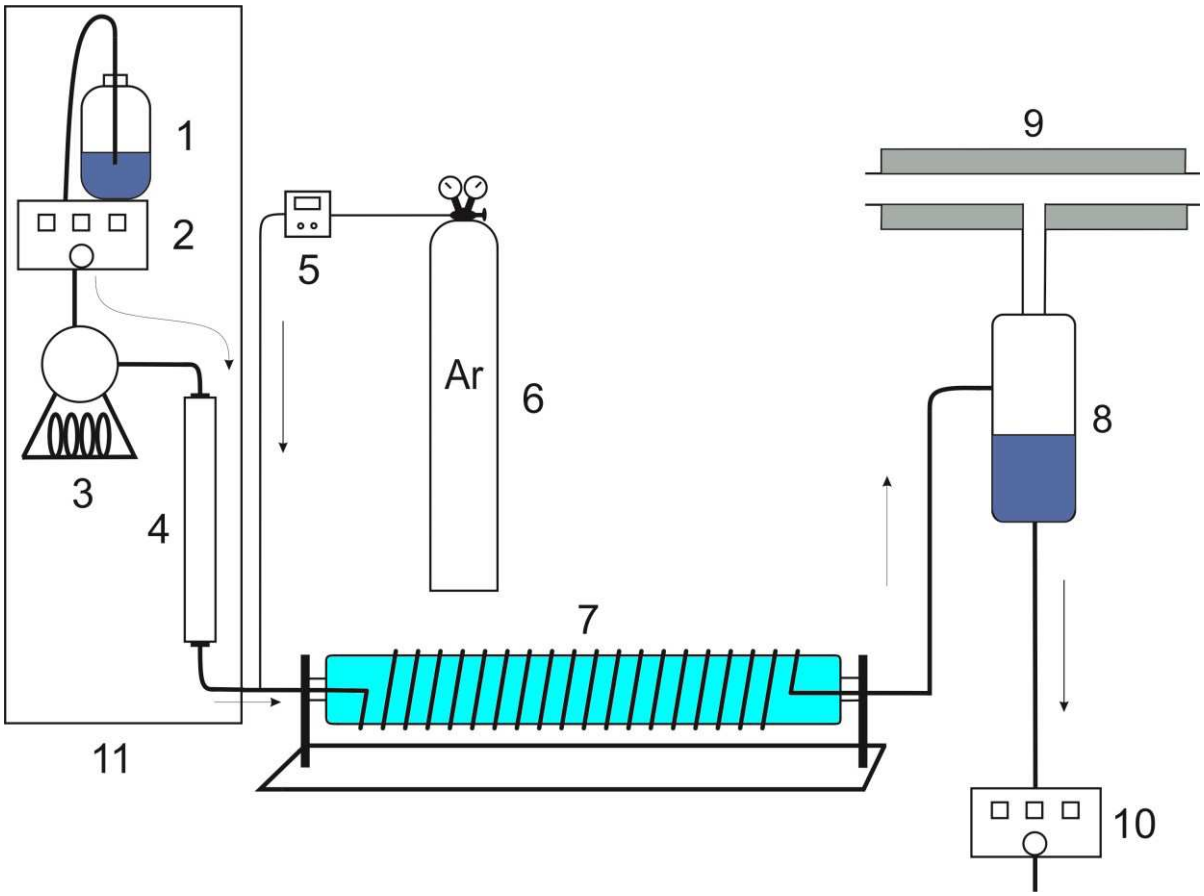

Fig. 1. The instrumental set-up used for mercury speciation analysis.

1-Mobile phase, 2-High-performance liquid chromatography pump, 3-Injection valve with loop, 4-Separation column, 5-Mass flow controller, 6-Cylinder with compressed argon, 7-Ultraviolet-photochemical reactor, 8-Gas-liquid separator, 9-Quartz detection tube, 10-Peristalic pump, 11-High-performance liquid chromatography system

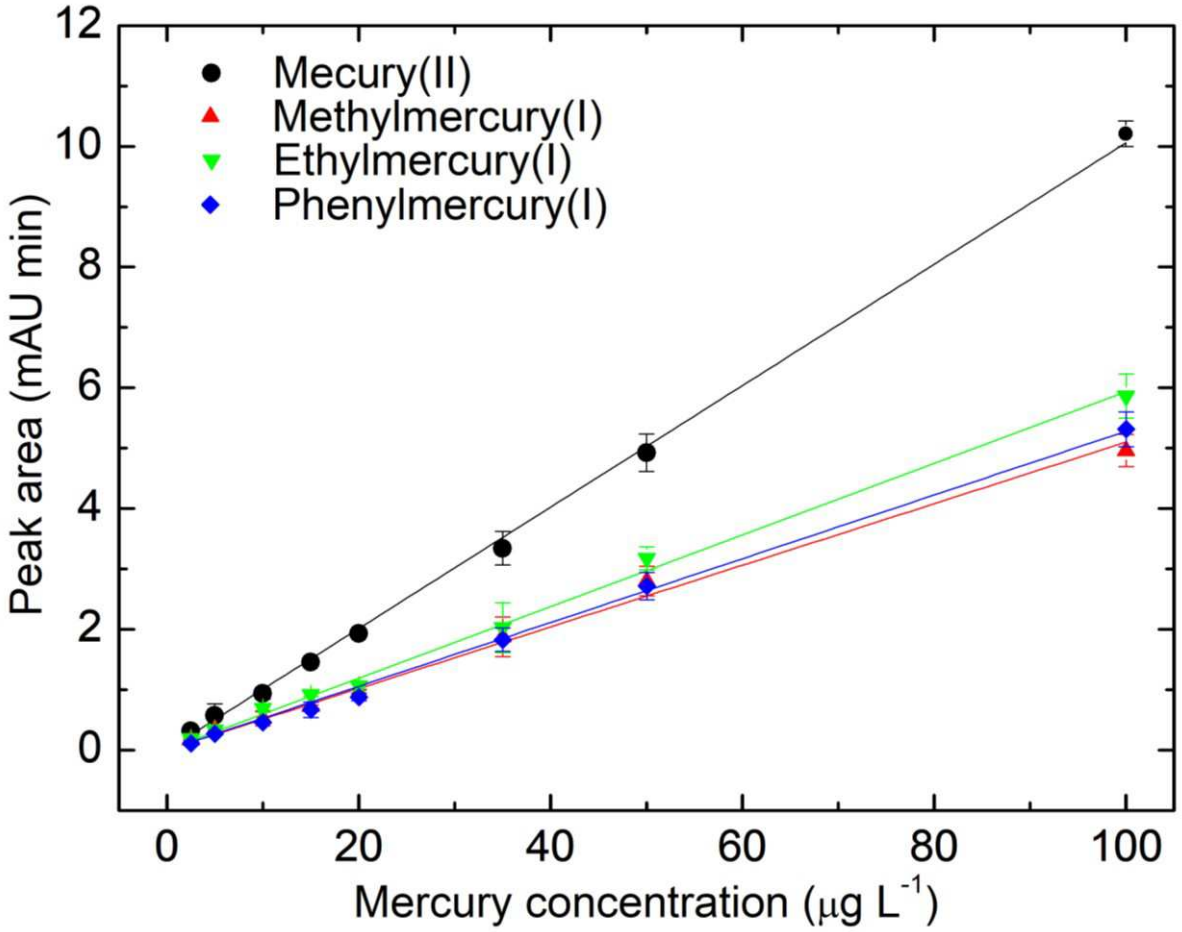

Fig. 2. Linear range of calibration curves attained by high-resolution continuum source-atomic absorption spectrometer for individual Hg species in a mixture. Mercury species standards in 20/20 mmol L^{-1} CH_3COOH/CH_3COONa, pH 4.75, 40% ethanol and 0.1% 2-mercaptoethanol. See Table 4 for experimental conditions.

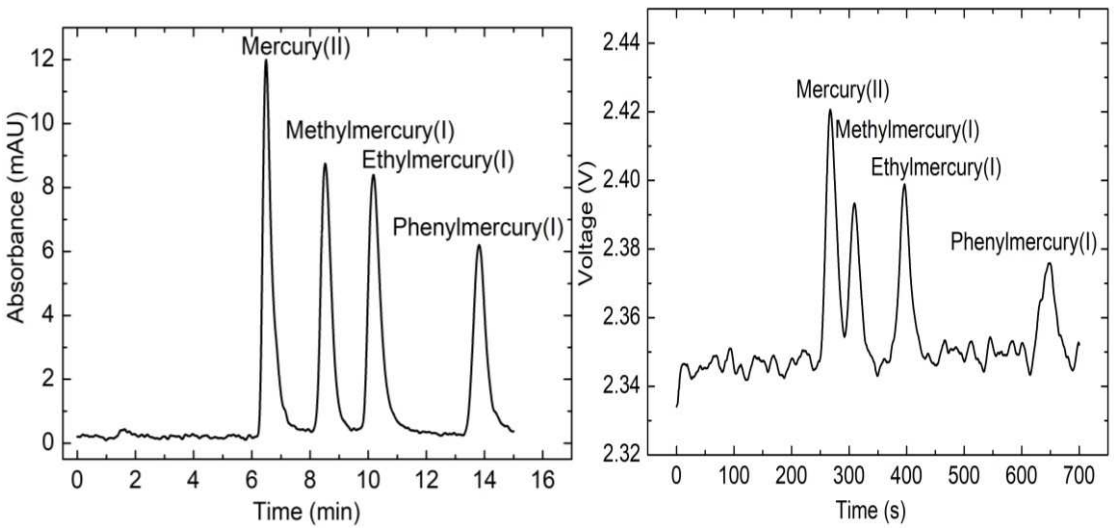

Fig. 3: The comparison of chromatograms (Hg concentration of each mercury species 50 µg L^{-1}) obtained under the optimum experimental conditions (Table 4).

Left: high-resolution continuum source-atomic absorption spectrometer; Phenomenex Gemini® column (3µm, 250 x 3 mm)

Right: Line-source-atomic absorption spectrometer; Phenomenex Gemini® column (3µm, 150 x 2.4 mm)